ROLES OF ANTICIPATION AND INERTIA IN ACTIVE ELASTIC SHEET MODELS

A THESIS SUBMITTED TO
THE GRADUATE SCHOOL OF NATURAL AND APPLIED SCIENCES
OF
MIDDLE EAST TECHNICAL UNIVERSITY

BY

MERT DEMIREL

IN PARTIAL FULFILLMENT OF THE REQUIREMENTS
FOR
THE DEGREE OF MASTER OF SCIENCE
IN
MECHANICAL ENGINEERING

NOVEMBER 2022

Approval of the thesis:

ROLES OF ANTICIPATION AND INERTIA IN ACTIVE ELASTIC SHEET MODELS

submitted by **MERT DEMIREL** in partial fulfillment of the requirements for the degree of **Master of Science in Mechanical Engineering Department, Middle East Technical University** by,

Prof. Dr. Halil Kalıpçılar
Dean, Graduate School of **Natural and Applied Sciences** _____

Prof. Dr. Mehmet Ali Sahir Arıkan
Head of Department, **Mechanical Engineering** _____

Assoc. Prof. Dr. Ali Emre Turgut
Supervisor, **Mechanical Engineering, METU** _____

Prof. Dr. Cristián Huepe
Co-supervisor, **ESAM, Northwestern University, USA** _____

Examining Committee Members:

Assoc. Prof. Dr. Ahmet Buğra Koku
Mechanical Engineering, METU _____

Assoc. Prof. Dr. Ali Emre Turgut
Mechanical Engineering, METU _____

Prof. Dr. Cristián Huepe
ESAM, Northwestern University, USA _____

Assoc. Prof. Dr. Ender Yıldırım
Mechanical Engineering, METU _____

Assist. Prof. Dr. Kutluk Bilge Arıkan
Mechanical Engineering, TED University _____

Date: 24.11.2022

I hereby declare that all information in this document has been obtained and presented in accordance with academic rules and ethical conduct. I also declare that, as required by these rules and conduct, I have fully cited and referenced all material and results that are not original to this work.

Name, Surname: Mert Demirel

Signature :

ABSTRACT

ROLES OF ANTICIPATION AND INERTIA IN ACTIVE ELASTIC SHEET MODELS

Demirel, Mert
M.S., Department of Mechanical Engineering
Supervisor: Assoc. Prof. Dr. Ali Emre Turgut
Co-Supervisor: Prof. Dr. Cristián Huepe

November 2022, 73 pages

The use of Active Matter (AM) concepts in robotics so as to model collective motion has become very prevalent, with Active Elastic Sheet (AES) models being the most recent ones. In this thesis, anticipation and inertial effects are introduced as the modifying AES parameters prior to multiple allocation studies. It is shown that anticipation behaves similar to damping under certain conditions, and inertial effects introduce a dynamical relaxation equivalent to a proportional velocity controller. Since velocities cannot instantly reach desired values due to the proportional gain, agents respond as if they have inertias. Rotational inertia is also investigated as the interception of instant alignment change apart from mass effects along the velocity vector. Reduced active matter models that utilizes two-particle versions of AES are developed in the pursuit of simpler representations for multi-agent systems. Toy models with both anticipation and inertial effects promise better preliminary studies for swarm robotics applications as they become more and more complex. A multi-agent simulator is built and several scenarios are functionalized in order to assess performance of toy models by comparison. Metrics such as damping ratio and agent separation are studied to discover

behavioural similarities between reduced and full models. Such similarities could enable simpler parameter tuning procedures applied on reduced toy models by extrapolating to multi-agent systems more practically. All experiments focus on tuning of anticipation as the control parameter for which order-disorder transition comparisons are carried out in order to understand its gradual effect. The relation between mass included analytical AM models and engineering controllers is justified with reduced versions of AES and phase transition studies under the measure of polarization.

Keywords: Swarm Robotics, Collective Motion, Anticipation, Inertial Effects

ÖZ

AKTİF ELASTİK LEVHA MODELLERİNDE ÖNGÖRÜNÜN VE ATALETİN ROLLERİ

Demirel, Mert
Yüksek Lisans, Makina Mühendisliği Bölümü
Tez Yöneticisi: Doç. Dr. Ali Emre Turgut
Ortak Tez Yöneticisi: Prof. Dr. Cristián Huepe

Kasım 2022 , 73 sayfa

Aktif Elastik Levha (AEL) modelleri en güncellerinden olmak üzere, Aktif Madde (AM) konseptlerinin kolektif hareketleri modellemek adına robotik alanda kullanımı yaygınlaşmış bulunmaktadır. Bu tezde, öngörü ve atalet etkileri çeşitli yerleşim çalışmaları öncesinde değiştirici AEL parametreleri olarak tanıtılmıştır. Öngörünün belirli şartlar altında sönümlemeye benzer davrandığı gösterilmiş, ve atalet etkileri oransal bir hız kontrolcüsüne eşdeğer olarak dinamik bir yavaşlatma sağlamıştır. Hızlar istenilen değerlere oransal kazanım nedeniyle anında ulaşamadığından ajanlar ataletleri varmış gibi davranmaktadır. Hız vektörü doğrultusunda etki gösteren kütlenin yanı sıra, anlık yön değişimlerini önlemek adına dönme ataleti de araştırılmıştır. Çok-ajanlı sistemlerin daha basit temsilleri amacıyla AELnın iki-parçacıklı versiyonlarını kullanan indirgenmiş aktif madde modelleri geliştirilmiştir. Öngörü ve atalet etkilerine sahip oyuncak modeller giderek daha da zorlayıcı hale evrilen sürü robotiği uygulamaları için daha iyi ön çalışmalar vadetmektedir. Oyuncak modellerin performansını karşılaştırmalı olarak değerlendirmek adına çok-ajanlı bir simülatör oluşturulmuş ve

çeşitli senaryolar işlevselleştirilmiştir. İndirgenmiş ve tam modeller arasındaki davranışsal benzerlikleri keşfetmek adına sönümleme oranı ve ajanlar arası boşluk esaslı metrikler incelenmiştir. Bu tür benzerlikler, indirgenmiş oyuncak modellerinde uygulanan daha basit parametre ayarlama prosedürlerini çok-ajanlı sistemlere daha pratik bir şekilde uyarlamayı mümkün kılabilecektir. Tüm deneyler, kademeli etkisi düzenli-düzensiz değişim karşılaştırmaları ile anlaşılmaya çalışılan öngörü kontrol parametresinin ayarlanmasına odaklanmıştır. Kütle içeren analitik AM modelleri ile mühendislik kontrolcüleri arasındaki ilişki, AELnın indirgenmiş versiyonları ve kutuplaşma ölçümlü faz değişimi çalışmaları ile doğrulanmıştır.

Anahtar Kelimeler: Sürü Robotiği, Kolektif Hareket, Öngörü, Atalet Etkileri

To My Beloved Ones

ACKNOWLEDGMENTS

I would like to thank my dear supervisor Assoc. Prof. Dr. Ali Emre Turgut for his valuable guidance throughout my graduate studies. He has always been involved in my development and helped me keep my health intact.

My dear co-supervisor Prof. Dr. Cristián Huepe has always been the very inspiring companion regardless of the distances in between. I would like to thank him for all of his support.

I have been kept motivated thanks to the generous support by TÜBİTAK with their 2211 Domestic Graduate Scholarship Programme (*2210-A General Domestic Post-Graduate Scholarship Programme*).

My friend İhsan Caner Boz shared his knowledge and experience from his own thesis studies without any hesitance. I am very grateful for his contributions to the *anticipation* part of this study.

Ersin Keskin has been the sole keyboard fellow through the most challenging simulation studies. I was very pleased to work with him and his extended coding knowledge has always shed a light on our long discussions we had together.

My parents Mehmet Demirel & Gülnaz Demirel, my sister Merve Demirel and my love Hatice Elif Tola have always been there for me whenever I needed them with their unconditional compassion and support. I would like to express my sincerest gratitude to them.

TABLE OF CONTENTS

ABSTRACT v

ÖZ vii

ACKNOWLEDGMENTS x

TABLE OF CONTENTS xi

LIST OF TABLES xiv

LIST OF FIGURES xv

LIST OF ABBREVIATIONS xviii

CHAPTERS

1 INTRODUCTION 1

1.1 Overview of the Study 1

1.2 Objective of the Thesis 2

2 LITERATURE SURVEY 5

2.1 Active Matter (AM) Concepts and Collective Motion 5

2.2 Emergence and Swarm Intelligence 6

2.3 Active Elastic Sheet (AES) Models 7

2.4 Swarm Robotics Applications 8

2.5 Contribution of the Thesis 8

3 METHODOLOGY 11

3.1 Active Elastic Sheet (AES) - The Simplest Model 11

3.2 Active Elastic Alignment (AEA) Model 13

3.3 Active Elastic Anticipation (AEAnt) Model 15

3.4 Inertia and Proportional Velocity Controller 16

4 ANALYTICAL DESCRIPTION 19

4.1 Overview of the Analytical Models 19

4.2 Two-Particle AE Models: Head-to-Tail Configuration 20

4.2.1 Head-to-Tail in 1st Order w/o Anticipation 20

4.2.2 Head-to-Tail in 1st Order w/ Anticipation 21

4.2.3 Head-to-Tail in 2nd Order w/o Anticipation 22

4.2.4 Head-to-Tail in 2nd Order w/ Anticipation 23

4.3 Two-Particle AE Models: Side-by-Side Configuration 24

4.3.1 Side-by-Side in 1st Order w/o Anticipation 24

4.3.2 Side-by-Side in 1st Order w/ Anticipation 25

4.3.3 Side-by-Side in 2nd Order w/o Anticipation 27

4.3.4 Side-by-Side in 2nd Order w/ Anticipation 28

5 NUMERICAL EXPERIMENTS 31

5.1 Performance Metrics 31

5.2 Experimental Setups 32

5.3 Multi-Agent Simulator 33

6 RESULTS & DISCUSSION 39

6.1 Similarities between AEA and AEAnt 39

6.2 Eigenvalue Plots for Toy Models 40

6.3 Toy Models vs. Multi-Agent Simulator 46

6.4 Avoidance Performance 49

6.5 Phase Diagrams 56

6.5.1 Phase Diagrams with Inertial Effects 59

7 CONCLUSION 65

7.1 Future Work 66

REFERENCES 69

LIST OF TABLES

TABLES

Table 5.1 Numerical Inputs Used in Multi-Agent Simulator 35

Table 5.2 Boolean Inputs Used in Multi-Agent Simulator 35

Table 6.1 System of Linearized Equations for AEA vs. AEAnt 39

Table 6.2 Distance between Two-Particles for Head-to-Tail Toy Models 49

Table 6.3 Distance between Two-Particles for Side-by-Side Toy Models 49

LIST OF FIGURES

FIGURES

Figure 3.1 Small Position and Orientation Perturbations for Stability Analysis of AES [1] 12

Figure 3.2 Small Position and Orientation Perturbations for Stability Analysis [2] 13

Figure 3.3 Small Position and Orientation Perturbations for Stability Analysis of AEA [2] 14

Figure 3.4 Proportional Velocity Controller 16

Figure 4.1 Head-to-Tail Configuration for Two-Particle AE 20

Figure 4.2 Side-by-Side Configuration for Two-Particle AE 24

Figure 5.1 Enabled Circular Ducts and Wall 36

Figure 5.2 Demonstration of Periodic Boundary Conditions 37

Figure 6.1 Eigenvalue Plots as a Function of Anticipation for Head-to-Tail Configuration in both 1st and 2nd Orders 41

Figure 6.2 Plot of $\lambda_i(m)$ from Eqn. (4.25) for Head-to-Tail Configuration in 2nd Order 42

Figure 6.3 Plot of $\lambda_i(b)$ from Eqn. (4.51) for Side-by-Side Configuration in 1st Order 42

Figure 6.4 Eigenvalue Plots as a Function of Anticipation for Side-by-Side Configuration in 2nd Order 43

Figure 6.5 Eigenvalue Plots as a Function of Mass for Side-by-Side Configuration in 2nd Order 44

Figure 6.6 Eigenvalue Plots as a Function of Rotational Inertia for Side-by-Side Configuration in 2nd Order 45

Figure 6.7 Agent Orientation vs. Time in a Multi-Agent System w/ Anticipation 47

Figure 6.8 Damping Trends for Toy Model vs. Multi-Agent System 48

Figure 6.9 Typical Duct Passage 51

Figure 6.10 Minimum and Maximum Distances in a Typical Duct Passage . . 52

Figure 6.11 Average Distance in a Typical Duct Passage 53

Figure 6.12 Typical Wall Bounce 53

Figure 6.13 Minimum and Maximum Distances in a Typical Wall Bounce . . 54

Figure 6.14 Average Distance in a Typical Wall Bounce 55

Figure 6.15 Duct Passage Failure 55

Figure 6.16 Order vs. Noise for Different Anticipation Values with $N = 127$ and Initially: Random 57

Figure 6.17 Order vs. Noise for Different Anticipation Values with $N = 127$ and Initially: Random vs. Ordered 58

Figure 6.18 Order vs. Noise for Different Anticipation Values with $N = 127$ vs. $N = 271$ and Initially: Random 58

Figure 6.19 Order vs. Noise with Various Anticipation Degrees for Different Rotational Inertia Values 60

Figure 6.19 Order vs. Noise with Various Anticipation Degrees for Different Rotational Inertia Values (Cont.) 61

Figure 6.20 Order vs. Noise with Various Rotational Inertia Values for Different Anticipation Degrees 62

Figure 6.20 Order vs. Noise with Various Rotational Inertia Values for Different Anticipation Degrees (Cont.) 63

Figure 6.21 Order vs. Noise with $I = 100$ for Different Anticipation Values . 64

LIST OF ABBREVIATIONS

2D	2 Dimensional
3D	3 Dimensional
AE	Active Elastic
AEA	Active Elastic Alignment
AEAnt	Active Elastic Anticipation
AES	Active Elastic Sheet
AM	Active Matter
BM	Boids Model
CAS	Complex Adaptive System
COR	Center-of-Rotation
CPS	Cyber-Physical System
DOF	Degree-of-Freedom
MAS	Multi-Agent System
PSO	Particle-Swarm Optimization
SI	Swarm Intelligence
SPP	Self-Propelled Particle
SS	Steady-State
VM	Vicsek Model

CHAPTER 1

INTRODUCTION

1.1 Overview of the Study

Active Matter (AM) concepts and collective motion have a deep connection by means of their underlying physics. From molecular scales of active solids/crystals up to macroscopic flock of birds, multi-agent models become powerful tools so as to investigate inner workings of interactions. Parameters such as scalability, decentralization, emergence, etc. come into prominence when a network of agents is built with relatively many connections. In a world where complexity equalize to more computational power, such emergent patterns promises simpler units performing challenging tasks that none of the constituent individuals can handle. This realm of collective motion has its extension to engineering applications, specifically in swarm robotics. From this standpoint, Active Elastic (AE) models build probably the most relevant bridge in between through their simplicities and characteristics. Throughout the thesis, AE models are used as the study of multi-agent systems.

AE models are open to a great number of modifications. Additional inter-connection parameters, various network topologies and cantilevered connections with offsets are among the possible extensions that are discussed in the upcoming chapters. For instance, Active Elastic Anticipation (AEAnt) models reveal great amount of new sights by introducing nature-like behaviours. As shown by Gerlee et al. [3], the existence of prediction regarding the positions of adjacent agents results in more stable collective motion as in the case of crystalline textures, and may even yield flocks' milling behaviour independent from the presence of self-propulsion. In addition to behavioural similarities, it is shown in the following chapters that different modifications may

even result in equivalent physics with the same mathematical expressions, yet different parameter selections. These kind of equivalences bring confidence for the development of reduced physics that would shed a light to the foundations in common. Reduced systems are powerful especially when the philosophy behind them is derived from the concept of *downward causation* [4]. Therefore, building a useful toy model for multi-agent systems is nothing but a significant part of the study that is given coverage by this thesis. The developed toy models are examined with several modifications and their stance in swarm applications. Various performance metrics are introduced for not only quantitative comparisons but also phase transition studies. The results are reflected from a swarm robotics engineering perspective.

1.2 Objective of the Thesis

The motivation behind AE modifications in this thesis focuses mainly on anticipation and inertia. The first step is to develop toy models with reduced two-particle AE versions. Having a base model with required simplifications, anticipation and inertial effects are to be added as the enriching parameters. A multi-agent simulator is required for a scalability assessment of toy model parameters. Hence, we find that an input driven simulator development becomes a necessity where number of agents, anticipation degree, inertial effects, perturbations, obstacles, etc. are all configurable by means of either a value or an on/off state. Rest of the study boils down to exhaustive set of experiments which demonstrate several performance measures ranging from scalability up to emergent characteristics.

The first *Introduction* chapter is followed by *Literature Survey* in which a deep journey from AM concepts up to macroscopic swarming applications are summarized with proper collocation. The journey is supported with emergence philosophy and its extensions to engineering implementations.

The third *Methodology* chapter elaborates current models with their core formalizations. Given methodologies from the literature also create a basement for the supervening *Analytical Description* chapter. Here, reduced two-particle AE models are derived with all the kinematic/kinetic details.

The fifth *Numerical Experiments* chapter is filled with handful of simulations where each and every comparison is illustrated properly in order to evaluate models' performance. All setups are described and portrayed in accordance with their experimental objectives. Outcomes are discussed thoroughly in the following *Results & Discussion* chapter.

Finally, the *Conclusion* chapter finalizes the study and investigates possible future work by expanding on what can be done further.

CHAPTER 2

LITERATURE SURVEY

2.1 Active Matter (AM) Concepts and Collective Motion

Active Matter (AM) is a collection of agents with active energy consumptions through exerted forces and individual movements. These systems are inherently not in equilibrium with their surroundings. AM concepts with the inclusion of self-dynamism are well related to the patterns observed in nature by means of collective motion. The underlying common principle is pronounced especially when Self-Propelled Particles (SPPs) are the reason for mentioned self-dynamism. Generalized patterns such as order of phases and long wave characteristics are already among common studies as in the case of work by Aditi Simha et al. [5]. At the core of all these studies, Vicsek Model (VM) [6] is the pioneering origin in which velocity-based alignment information is shared by the neighbourhood of each agent. The common interest in collective motion studies is generally the phase transition. For instance, Aldana et al. [7] investigate long-range interactions with a network-approach in the pursuit of ordered to disordered state transitions. Such critical points as a result of discontinuous transition states exist even in the simplest form of VM [8, 9]. These transitions appear at an emergent scale ranging from crystals [10] up to living organisms such as tissue cells [11] if not macroscopic swarms. As the other way around, *downward causation* [4] is well appreciated by Peshkov et al. [12] such that interactions with metric-free topologies in natural swarms are worth being traced down to AM systems as how their study shows.

2.2 Emergence and Swarm Intelligence

The causation between AM systems and collective motion is predicated on the concept of emergence. Although Multi-Agent System (MAS) is described by the lower level components and Complex Adaptive System (CAS) is described as the higher level phenomena, they are definitions for the same system with a common goal: *an intelligent organization out of simple constituents* [13]. Such definition of emergence promises a great potential for more efficient ways of creating building blocks.

The same building block throughout the whole system with simple local rules can define a collective motion once such rules are determinant enough as in the case of Boids Model (BM) [14], the ancestor of VM. A flock can be easily simulated in BM once below-given set of simple rules are applied by each and every agent.

- *Collision Avoidance:* Agents avoid colliding with neighbours.
- *Velocity Matching:* Agents match their velocities with that of neighbours.
- *Flock Centering:* Agents try to stay as close as possible to neighbours.

The alignment-based VM has similar set of simple rules and agents need to match their orientations with that of neighbours [6]. VM can still procure collective motion in the absence of a leader [15]. Yet similar behaviour is valid when endocannibalism is the case with agent-based escape and pursuit responses [16]. All these effects are very well existent in natural swarms as how Vicsek et al. [17] picture in their study.

These kind of emergent behaviours from an aggregation of simplistic elements reveal an intelligence that none of the agents themselves individually have. In other words, such behaviours turn out to be *irreducible* [4]. Intelligence being a broad definition, Swarm Intelligence (SI) is a specific contemporary field with yet to be frame-worked [18]. Schranz et al. [19] picture another outline pivoted around Cyber-Physical Systems (CPSs) in addition to the one proposed in [18]. Swarm size as a performance measure becomes a metric when advantages such as adaptability and scalability of swarms get used in the way CPSs utilize SI systems. In that sense, swarm size change can be further deepened with conceptual discussions such as *autopoiesis* [20]. In this thesis, studies are based on fixed number of agents where toy

models are represented with reduced static swarm sizes. For a fixed swarm size, emergence can be studied in both micro and macro levels [21], *downward causation* being the micro one. There have been studies where experimental data is used in order to determine agent interactions downward to the micro level [22], [23]. Yet, macroscopic formations (such as vortices and migrations [24]) are among more common studies after fitting individual-level parameters. The way this thesis proposes toy models is based on downward direction not in the sense of interactions, but the reduction of fixed swarm size. Seeing similar patterns in smaller swarms with that of larger versions is still nothing but an extension of the *downward causation* concept.

2.3 Active Elastic Sheet (AES) Models

AES models are AM systems described in 2-Dimensional (2D) planes with the simplistic spring-like interactions in between the constituent agents. Unlike AES, velocity-based VM utilizes alignment/orientation as the information share in between agents. Ferrante et al. [25,26] show that a position-based model with SPPs can employ collective rotation/translation states without any information of orientation sharing. Model is based on a swarm with agents that substitute particles in AES under rotational and translational degree-of-freedoms (DOFs), and their information sharing with adjacent agents is utilized by the spring forces between AES nodes as functions of positions. Such configuration of model is on par with semi-rigid AM concepts. Therefore, it is showed that phase transitions are also eminent in AES just as in the case of prior AM concepts with SPPs.

Various modifications exist for AE models. Turgut et al. [27] study different network topologies among the agents for both AE and Vicsek models as a fundamental alteration. Three types of connectivities are investigated: *NN:* Nearest-Neighbour, *ER:* Erdös–Rényi, *SF:* Scale-Free and super-positions of them. Critical phase transition levels are examined for different interaction networks.

Yet another modification over the simple AES is by Lin et al. [2] such that the agents are attached by the interacting springs in a cantilevered manner, at a distance R in front of their center-of-rotations (CORs). Phase transitions are investigated similar to

the work of network topologies, yet both locally and globally this time.

2.4 Swarm Robotics Applications

Emergent SI means simpler building blocks that bring an efficiency for task allocation. This is nothing but an engineering dream which enables simpler designs with much better performance by means of applications. Hence, there have been a lot of review studies about swarm robotics lately [28–33]. Each work presents a different taxonomy with varying frame-works, yet common categorizations exist. This is an expected situation since swarm robotics include a broad range of engineering applications from Particle-Swarm Optimizations (PSOs) up to real-world agent robots.

Evolutionary methods are well prominent when it comes to *downward causation*: given a task, configure agent behaviours... From Novelty-Search methods [34] to Neural-Network controllers [35], there exist several studies aiming at evolutionary robotics in swarms. Among all of them, the method called *Turing Learning* is the most relevant one in terms of micro-level controller design [36–40]. *Turing Learning* can find impressively simple controllers so as to perform the desired tasks. Ferrante et al. [41] appreciate the importance of simple input/output relations by studying robots with and without certain parameters such as the orientation control in flocking. Considering what these flocks of flying robots are capable of [42, 43], concepts that make certain sensory inputs/controllers redundant are at great importance due to their efficient nature. Hence, AE models carry high potentials for swarm robots applications when alignment share and control are rendered unnecessary. There already exist studies in which AES is used as the underlying model for swarm robots, just as in the case of *Mona* by Raoufi et al. [44]. It is also worthwhile to assess capabilities of position-based control methods for certain limitations as worked out by Zheng et al. [1].

2.5 Contribution of the Thesis

In this thesis, further AES modifications are investigated. New parameters are introduced prior to the development of toy models for multi-agent AES. Reduced two-

particle systems are chosen to be base models for the simplified versions of AES with N-many agents. Reducing dimensions and swarm sizes down to the least possible values results in simpler extrapolation processes for further multi-agent analysis. To illustrate, Czirók et al. [45] study SPP models down to 1D in order to determine order-disorder transitions as a larger model validation. In a similar manner, reduced two-particle systems of AE models with different configurations are studied for common behaviours, specifically the stability characteristics.

The expected similarities in patterns include common behaviours for anticipation and inertia terms. An anticipating agent can extrapolate the future positions of other agents. Such inclusion of prediction stabilizes the system and results in ordered states as AM models. All these effects are well-studied by Gerlee et al. [3] on dynamical systems. In this thesis, AES is not only modified with anticipating terms but also introduced with inertial effects along both translational and rotational axes. Addition of inertia turns out to relax underlying dynamics and behave as if a proportional velocity controller exists. Stabilization due to inertial effects prevents instant disrupt changes in kinematic parameters. It is also shown that different kinds of equivalences exist between the developed toy models. For instance, AEA and AEAnt turn out to be expressed the same by means of mathematical formulation, yet different parameter selections.

A multi-agent simulator is built in MATLAB with configurable variables. Conditions such as inclusion of noise/perturbations, obstacles, bouncing walls, etc. are all defined as a boolean parameter in an on/off state manner. Using multi-agent system simulators, toy models are tested in terms of their emergent performance specifically based on the scalability. Similar patterns in their damping responses are sought. The study is finalized after extensive order-disorder studies are carried out using the simulator.

CHAPTER 3

METHODOLOGY

3.1 Active Elastic Sheet (AES) - The Simplest Model

The simplest form of AE models is AES where agents are connected to each other by spring-like interactions in a 2D plane [25, 26]. System of N agents are described by the below-given over-damped equations of motion.

$$\dot{\vec{x}}_i = v_0 \hat{n}_i + \alpha[(\vec{F}_i + D_r \hat{\xi}_r) \cdot \hat{n}_i]\hat{n}_i \tag{3.1}$$

$$\dot{\theta}_i = \beta[(\vec{F}_i + D_r \hat{\xi}_r) \cdot \hat{n}_i^{\perp}] + D_\theta \xi_\theta \tag{3.2}$$

Here,

- $\dot{\vec{x}}_i$: Linear velocity of each agent i
- $\dot{\theta}_i$: Angular speed of each agent i
- v_0: Self-propulsion or forward biasing speed
- α: Inverse translational damping coefficient
- β: Inverse rotational damping coefficient
- $\hat{n}_i$: Unit vector parallel to the heading direction of each agent i
- $D_r \hat{\xi}_r$: *Sensing noise* (force measurement errors) with the noise strength coefficient of D_r and a random unit vector $\hat{\xi}_r$
- $D_\theta \xi_\theta$: *Actuation noise* (individual motion fluctuations) with the noise strength coefficient of D_θ and a random variable ξ_θ with a uniform distribution

The total force acting on each agent i is nothing but the sum of all spring forces.

$$\vec{F}_i = \sum_{j \in S_i} -\frac{k}{l_{ij}}(||\vec{r}_{ij}|| - l_{ij})\frac{\vec{r}_{ij}}{||\vec{r}_{ij}||} \tag{3.3}$$

where,

$$\vec{r}_{ij} = \vec{x}_j - \vec{x}_i \tag{3.4}$$

with free lengths of l_{ij} and spring constants k/l_{ij}.

Equations of AES can easily be converted to numerical versions by Euler method discretization.

$$\vec{x}_i^{t+1} = \vec{x}_i^t + \left\{ v_0 \hat{n}_i + \alpha \left[\left(\vec{F}_i^t + \frac{D_r}{\sqrt{\Delta t}} \hat{\xi}_r \right) \cdot \hat{n}_i \right] \hat{n}_i \right\} \Delta t \tag{3.5}$$

$$\theta_i^{t+1} = \theta_i^t + \left\{ \beta \left[\left(\vec{F}_i^t + \frac{D_r}{\sqrt{\Delta t}} \hat{\xi}_r \right) \cdot \hat{n}_i^{\perp} \right] + \frac{D_\theta}{\sqrt{\Delta t}} \xi_\theta \right\} \Delta t \tag{3.6}$$

Divisions by $\sqrt{\Delta t}$ is proposed so as to prevent noise accumulations.

For stability analysis of AES, small perturbations are considered. For simplicity, a symmetric boundary condition for a two-particle system is constructed. Therefore, agents behave the mirrored versions of each others motion.

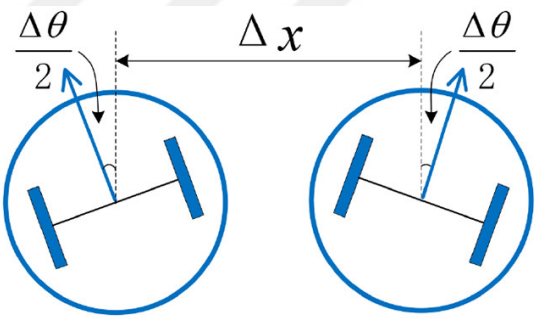

Figure 3.1: Small Position and Orientation Perturbations for Stability Analysis of AES [1]

Zheng et al. [1] calculates how these perturbations evolve by time using equations of motion in order to assess the linearized stability of the system (see Figure 3.1).

$$\frac{d}{dt}\Delta x = 2\left(v_0 - \alpha k \Delta x \sin\frac{\Delta\theta}{2}\right)\sin\frac{\Delta\theta}{2} \tag{3.7}$$

$$\frac{d}{dt}\Delta\theta = -2\beta k \Delta x \cos\frac{\Delta\theta}{2} \tag{3.8}$$

Linearization of Eqns. (3.7) and (3.8) for very small perturbations under small-angle approximation gives the below system of linearized equations.

$$\frac{d}{dt}\begin{Bmatrix}\Delta x\\ \Delta\theta\end{Bmatrix}=\begin{bmatrix}0 & v_0\\ -2\beta k & 0\end{bmatrix}\begin{Bmatrix}\Delta x\\ \Delta\theta\end{Bmatrix} \tag{3.9}$$

Eigenvalues calculated from the coefficient matrix of Eqn. (3.9) are indicative of the system stability. Hence,

$$\text{eig}\begin{pmatrix}0 & v_0\\ -2\beta k & 0\end{pmatrix}\rightarrow\boxed{\lambda_{\pm}=\pm\sqrt{-2\beta k v_0}} \tag{3.10}$$

One can easily note that both of the eigenvalues are purely imaginary and the system continuous its oscillations without any dampening out.

The procedure given above is the pioneering form of how the toy model stabilities are assessed through out this thesis.

3.2 Active Elastic Alignment (AEA) Model

Active Elastic Alignment (AEA) model is a modified version of AES with cantilevered arms for offset spring connections.

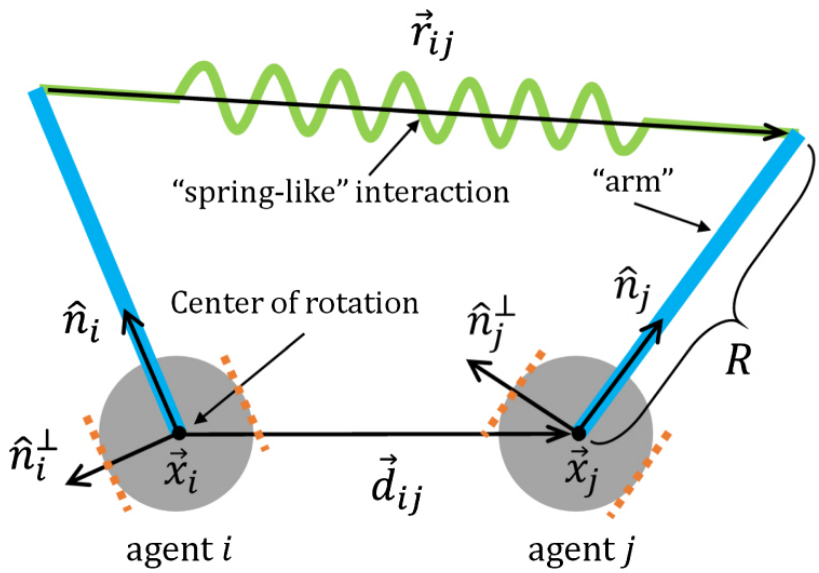

Figure 3.2: Small Position and Orientation Perturbations for Stability Analysis [2]

Lin et al. [2] study system of N agents with the same over-damped equations of motion by AES. The only difference comes into play due to the extending arms (see Figure 3.2). The effect of arm offset is utilized as a modification to the Eqn. (3.4).

$$\vec{r}_{ij} = (\vec{x}_j + R\hat{n}_j) - (\vec{x}_i + R\hat{n}_i) = \vec{x}_j - \vec{x}_i + R(\hat{n}_j - \hat{n}_i) \tag{3.11}$$

Here, R is length of the arm and $R = 0$ case is nothing but the good old AES model.

For stability analysis of AEA, small perturbations are considered again. For simplicity, a symmetric boundary condition for a two-particle system is constructed in a similar manner.

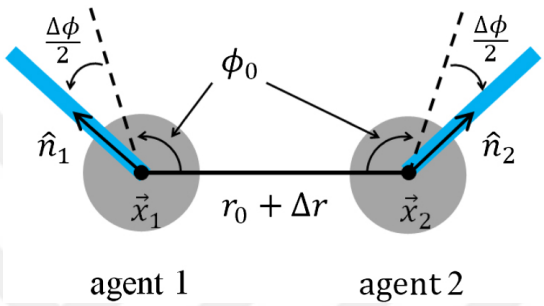

Figure 3.3: Small Position and Orientation Perturbations for Stability Analysis of AEA [2]

Lin et al. [2] calculates how these perturbations evolve by time using equations of motion in order to assess the linearized stability of the system (see Figure 3.3).

$$\frac{d}{dt}\Delta r = 2\left[v_0 - \alpha k\left(\Delta r + 2R\sin\frac{\Delta\phi}{2}\right)\sin\frac{\Delta\phi}{2}\right]\sin\frac{\Delta\phi}{2} \tag{3.12}$$

$$\frac{d}{dt}\Delta\phi = -2\beta k\left(\Delta r + 2R\sin\frac{\Delta\phi}{2}\right)\cos\frac{\Delta\phi}{2} \tag{3.13}$$

Linearization of Eqns. (3.12) and (3.13) for very small perturbations under small-angle approximation gives the below system of linearized equations.

$$\frac{d}{dt}\begin{Bmatrix}\Delta r\\ \Delta\phi\end{Bmatrix} = \begin{bmatrix}0 & v_0\\ -2\beta k & -2\beta kR\end{bmatrix}\begin{Bmatrix}\Delta r\\ \Delta\phi\end{Bmatrix} \tag{3.14}$$

Eigenvalues calculated from the coefficient matrix of Eqn. (3.14) are indicative of the system stability. Hence,

$$\text{eig}\begin{pmatrix}0 & v_0\\ -2\beta k & -2\beta kR\end{pmatrix} \rightarrow \boxed{\lambda_\pm = -\beta kR \pm \sqrt{\beta^2k^2R^2 - 2\beta kv_0}} \tag{3.15}$$

It is straight-forward to observe that $R = 0$ case results in exactly the same eigenvalues that of AES with persistent oscillations due to purely imaginary nature. For $R > 0$ and $v_0 < \beta k R^2/2$, both eigenvalues are real and negative with an over-damped decaying solution. For $R < 0$ and $v_0 > \beta k R^2/2$, on the other hand, both eigenvalues have negative real and imaginary parts. In that case, aligned state is achieved after damping certain amount of oscillations.

Lin et al. [2] also present a stability analysis for *Head-to-Tail* configuration of a two-particle system. It is observed that the solution in that case is always unstable.

3.3 Active Elastic Anticipation (AEAnt) Model

Active Elastic Anticipation (AEAnt) model is a modified version of AES with additional forcing terms that induces anticipation effect as if a damper is realized between agents. The only difference comes into play due to the additional forcing terms and this is utilized by performing a modification to the Eqn. (3.3).

$$\vec{F}_i = \sum_{j \in S_i} \left[-\frac{k}{l_{ij}} (||\vec{r}_{ij}|| - l_{ij}) - b||\vec{v}_{ij}|| \right] \frac{\vec{r}_{ij}}{||\vec{r}_{ij}||} \tag{3.16}$$

where,

$$\vec{v}_{ij} = \dot{\vec{r}}_{ij} \tag{3.17}$$

The parameter b is the anticipation level added to the spring interaction. It is again straight-forward to observe that $b = 0$ case results in exactly the same eigenvalues that of AES with persistent oscillations due to purely imaginary nature.

It is yet to be shown in the upcoming chapters that AEA and AEAnt have a lot of common mathematical expressions by means of different parameter representations such that $bv_0 \equiv kR$. In other words, spring interaction with a constant of k in AEA happens ahead of the COR as it is an elongated object with a distance R, yet AEAnt predicts future position corresponding to the same ahead destination with b weighted distance by the self propulsion of v_0.

3.4 Inertia and Proportional Velocity Controller

An engineering approach to AES based swarm robotics applications is prone to instant/abrupt kinematic changes as seen in [1,44]. One way to solve this issue is using a proportional velocity controller suggested by Bando et al. [46]. Their *Optimal Velocity Model* resolves the similar problem that occurs in traffic flows. With this model, cars cannot reach to their desired velocities instantly and need to accelerate in proportional accordance with the velocity difference between their current and target values.

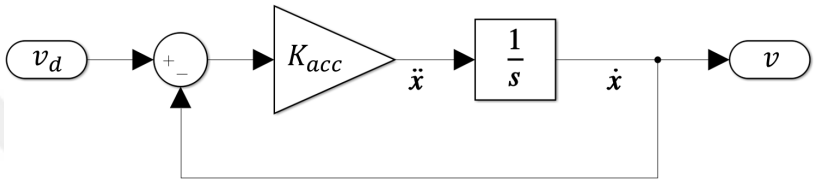

Figure 3.4: Proportional Velocity Controller

It is to be demonstrated below how such a controller used in AEAnt models is equivalent to the inclusion of inertia (see Figure 3.4).

$$v_d = v_0 - \alpha k \Delta x - \alpha b \Delta \dot{x} \tag{3.18}$$

$$\ddot{x} = K_{acc}(v_d - \dot{x}) \tag{3.19}$$

Plugging v_d expression in Eqn. (3.18) to Eqn. (3.19), we get a single line of equation to be handled.

$$\ddot{x} = K_{acc}(v_0 - \alpha k \Delta x - \alpha b \Delta \dot{x} - \dot{x}) \tag{3.20}$$

Rearranging Eqn. (3.20) gives the final form seen in AE(Ant) models, yet with an additional second order inertial term on the left.

$$\alpha m \ddot{x} + \dot{x} = v_0 - \alpha k \Delta x - \alpha b \Delta \dot{x} \quad \text{where} \quad \alpha m = \frac{1}{K_{acc}} \tag{3.21}$$

This is a valuable conclusion since it shows that adding a second order term to the left with an inertial coefficient is nothing but equivalent to a proportional velocity controller. This means AE models can be easily modified for both toy model studies and swarm robotics applications for a better representation of the real mass. It is

also straightforward to see that introducing rotational inertia to the angular part of AE models' equations of motion is a similar procedure as that of the given demonstration above.

CHAPTER 4

ANALYTICAL DESCRIPTION

4.1 Overview of the Analytical Models

In this chapter, it is aimed to derive analytical expressions for a system simple enough to observe and understand the effect of anticipation and inertia. Hence, reduced two-particle AE models are studied with small perturbations as how Zheng at al. [1] and Lin et al. [2] investigate small changes in degree-of-freedoms for stability analysis. Two models are presented: *Head-to-Tail* and *Side-by-Side* configurations. Over-damped equations of motions are used with four scenarios per configuration, which are listed below.

- 1st Order (w/o Inertia) and w/o Anticipation
- 1st Order (w/o Inertia) and w/ Anticipation
- 2nd Order (w/ Inertia) and w/o Anticipation
- 2nd Order (w/ Inertia) and w/ Anticipation

4.2 Two-Particle AE Models: Head-to-Tail Configuration

The configuration for head-to-tail two-particle AE model is given below.

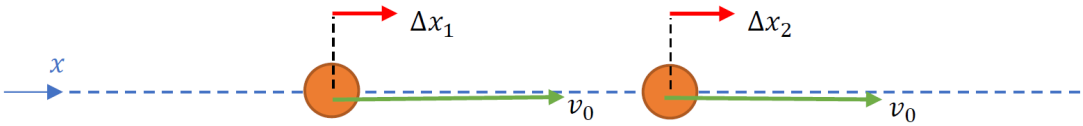

Figure 4.1: Head-to-Tail Configuration for Two-Particle AE

4.2.1 Head-to-Tail in 1st Order w/o Anticipation

Over-damped equations of motion are constructed below.

$$\Delta\dot{x}_1 = v_0 + \alpha k(\Delta x_2 - \Delta x_1) \tag{4.1}$$

$$\Delta\dot{x}_2 = v_0 - \alpha k(\Delta x_2 - \Delta x_1) \tag{4.2}$$

Then, the model in only first-order terms becomes a system of ODEs.

$$\begin{Bmatrix} \Delta\dot{x}_1 \\ \Delta\dot{x}_2 \end{Bmatrix} = \begin{bmatrix} -\alpha k & \alpha k \\ \alpha k & -\alpha k \end{bmatrix} \begin{Bmatrix} \Delta x_1 \\ \Delta x_2 \end{Bmatrix} \tag{4.3}$$

For stability analysis, eigenvalues of our system matrix are to be calculated.

$$\text{eig}\begin{pmatrix} -\alpha k & \alpha k \\ \alpha k & -\alpha k \end{pmatrix} \rightarrow \boxed{\lambda_- = -2\alpha k, \quad \lambda_+ = 0} \tag{4.4}$$

Eigenvalues reflect a marginally stable system regardless of the parameter selection. Absence of imaginary parts with all real values results in a non-oscillatory system.

Analytical solutions for positional perturbations can be easily expressed using above-calculated eigenvalues.

$$\Delta x_1 = v_0 t + C_1 - C_2 e^{-2\alpha k t} \tag{4.5}$$

$$\Delta x_2 = v_0 t + C_1 + C_2 e^{-2\alpha k t} \tag{4.6}$$

Finally, change in distance between the two particles can be expressed as the difference of calculated positional perturbations.

$$|\Delta x_1 - \Delta x_2| = |2C_2 e^{-2\alpha k t}| \tag{4.7}$$

4.2.2 Head-to-Tail in 1st Order w/ Anticipation

Over-damped equations of motion are constructed below.

$$\Delta\dot{x}_1 = v_0 + \alpha k(\Delta x_2 - \Delta x_1) + \alpha b(\Delta\dot{x}_2 - \Delta\dot{x}_1) \tag{4.8}$$

$$\Delta\dot{x}_2 = v_0 - \alpha k(\Delta x_2 - \Delta x_1) - \alpha b(\Delta\dot{x}_2 - \Delta\dot{x}_1) \tag{4.9}$$

Then, the model in only first-order terms becomes a system of ODEs.

$$\begin{Bmatrix} \Delta\dot{x}_1 \\ \Delta\dot{x}_2 \end{Bmatrix} = \begin{bmatrix} -\frac{\alpha k}{1+2\alpha b} & \frac{\alpha k}{1+2\alpha b} \\ \frac{\alpha k}{1+2\alpha b} & -\frac{\alpha k}{1+2\alpha b} \end{bmatrix} \begin{Bmatrix} \Delta x_1 \\ \Delta x_2 \end{Bmatrix} \tag{4.10}$$

For stability analysis, eigenvalues of our system matrix are to be calculated.

$$\text{eig}\begin{pmatrix} -\frac{\alpha k}{1+2\alpha b} & \frac{\alpha k}{1+2\alpha b} \\ \frac{\alpha k}{1+2\alpha b} & -\frac{\alpha k}{1+2\alpha b} \end{pmatrix} \rightarrow \boxed{\lambda_- = -\frac{2\alpha k}{1+2\alpha b}, \quad \lambda_+ = 0} \tag{4.11}$$

Again, eigenvalues reflect a marginally stable system regardless of the parameter selection, yet with an additional anticipation term. Absence of imaginary parts with all real values results in a non-oscillatory system for this case as well.

Analytical solutions for positional perturbations can be easily expressed using above-calculated eigenvalues.

$$\Delta x_1 = v_0 t + C_1 - C_2 e^{-\frac{2\alpha k}{1+2\alpha b}t} \tag{4.12}$$

$$\Delta x_2 = v_0 t + C_1 + C_2 e^{-\frac{2\alpha k}{1+2\alpha b}t} \tag{4.13}$$

Finally, change in distance between the two particles can be expressed as the difference of calculated positional perturbations.

$$|\Delta x_1 - \Delta x_2| = |2C_2 e^{-\frac{2\alpha k}{1+2\alpha b}t}| \tag{4.14}$$

Here, we see that the inclusion of anticipation makes $|\Delta x_1 - \Delta x_2|$ decay slower to its steady-state value due to the $1/(1+2\alpha b)$ term in the exponent. Hence, anticipation introduces an additional control parameter.

4.2.3 Head-to-Tail in 2nd Order w/o Anticipation

Over-damped equations of motion are constructed below.

$$\alpha m\ddot{x}_1 + \Delta\dot{x}_1 = v_0 + \alpha k(\Delta x_2 - \Delta x_1) \tag{4.15}$$

$$\alpha m\ddot{x}_2 + \Delta\dot{x}_2 = v_0 - \alpha k(\Delta x_2 - \Delta x_1) \tag{4.16}$$

Introducing $\Delta\dot{x}_1 = \Delta u$ and $\Delta\dot{x}_2 = \Delta w$, the model in only first-order terms becomes a system of ODEs.

$$\begin{Bmatrix} \Delta\dot{x}_1 \\ \Delta\dot{x}_2 \\ \Delta\dot{u} \\ \Delta\dot{w} \end{Bmatrix} = \begin{bmatrix} 0 & 0 & 1 & 0 \\ 0 & 0 & 0 & 1 \\ -\frac{k}{m} & \frac{k}{m} & -\frac{1}{\alpha m} & 0 \\ \frac{k}{m} & -\frac{k}{m} & 0 & -\frac{1}{\alpha m} \end{bmatrix} \begin{Bmatrix} \Delta x_1 \\ \Delta x_2 \\ \Delta u \\ \Delta w \end{Bmatrix} \tag{4.17}$$

For stability analysis, eigenvalues of our system matrix are to be calculated.

$$\lambda_1 = 0, \quad \lambda_2 = -\frac{1}{\alpha m}, \quad \lambda_3 = \frac{-1-\sqrt{1-8\alpha^2 km}}{2\alpha m}, \quad \lambda_4 = \frac{-1+\sqrt{1-8\alpha^2 km}}{2\alpha m} \tag{4.18}$$

Eigenvalues reflect a marginally stable system regardless of the parameter selection since real parts can never become positive. As long as $1 < 8\alpha^2 km$, system is oscillatory with generated imaginary parts.

Analytical solutions for positional perturbations can be easily expressed using above-calculated eigenvalues.

$$\Delta x_1 = v_0 + C_4 e^{-\frac{1}{\alpha m}t} - C_2 e^{\frac{-1-\sqrt{1-8\alpha^2 km}}{2\alpha m}t} - C_3 e^{\frac{-1+\sqrt{1-8\alpha^2 km}}{2\alpha m}t} \tag{4.19}$$

$$\Delta x_2 = v_0 + C_4 e^{-\frac{1}{\alpha m}t} + C_2 e^{\frac{-1-\sqrt{1-8\alpha^2 km}}{2\alpha m}t} + C_3 e^{\frac{-1+\sqrt{1-8\alpha^2 km}}{2\alpha m}t} \tag{4.20}$$

Finally, change in distance between the two particles can be expressed as the difference of calculated positional perturbations.

$$|\Delta x_1 - \Delta x_2| = \left| 2C_2 e^{\frac{-1-\sqrt{1-8\alpha^2 km}}{2\alpha m}t} + 2C_3 e^{\frac{-1+\sqrt{1-8\alpha^2 km}}{2\alpha m}t} \right| \tag{4.21}$$

It is observed that an additional order in the system not only increases the amount of eigenvalues with extended dynamics but also introduces a new control parameter m, namely the spatial mass.

4.2.4 Head-to-Tail in 2nd Order w/ Anticipation

Over-damped equations of motion are constructed below.

$$\alpha m\ddot{x}_1 + \Delta\dot{x}_1 = v_0 + \alpha k(\Delta x_2 - \Delta x_1) + \alpha b(\Delta\dot{x}_2 - \Delta\dot{x}_1) \tag{4.22}$$

$$\alpha m\ddot{x}_2 + \Delta\dot{x}_2 = v_0 - \alpha k(\Delta x_2 - \Delta x_1) - \alpha b(\Delta\dot{x}_2 - \Delta\dot{x}_1) \tag{4.23}$$

Introducing $\Delta\dot{x}_1 = \Delta u$ and $\Delta\dot{x}_2 = \Delta w$, the model in only first-order terms becomes a system of ODEs.

$$\begin{Bmatrix} \Delta\dot{x}_1 \\ \Delta\dot{x}_2 \\ \Delta\dot{u} \\ \Delta\dot{w} \end{Bmatrix} = \begin{bmatrix} 0 & 0 & 1 & 0 \\ 0 & 0 & 0 & 1 \\ -\frac{k}{m} & \frac{k}{m} & \frac{-1-\alpha b}{\alpha m} & \frac{b}{m} \\ \frac{k}{m} & -\frac{k}{m} & \frac{b}{m} & \frac{-1-\alpha b}{\alpha m} \end{bmatrix} \begin{Bmatrix} \Delta x_1 \\ \Delta x_2 \\ \Delta u \\ \Delta w \end{Bmatrix} \tag{4.24}$$

For stability analysis, eigenvalues of our system matrix are to be calculated.

$$\lambda_1 = 0, \quad \lambda_2 = -\frac{1}{\alpha m}, \quad \lambda_3 = \frac{-1 - 2\alpha b - \sqrt{1 - 8\alpha^2 km + 4\alpha^2 b^2}}{2\alpha m}, \\ \lambda_4 = \frac{-1 - 2\alpha b + \sqrt{1 - 8\alpha^2 km + 4\alpha^2 b^2}}{2\alpha m} \tag{4.25}$$

Again, eigenvalues reflect a marginally stable system regardless of the parameter selection since real parts can never become positive. As long as $1 < (8\alpha^2 km - 4\alpha^2 b^2)$, system is oscillatory with generated imaginary parts for this case as well.

Analytical solutions for positional perturbations can be easily expressed using above-calculated eigenvalues.

$$\Delta x_1 = v_0 + C_4 e^{-\frac{1}{\alpha m}t} - C_2 e^{\frac{-1-2\alpha b-\sqrt{1-8\alpha^2 km+4\alpha^2 b^2}}{2\alpha m}t} - C_3 e^{\frac{-1-2\alpha b+\sqrt{1-8\alpha^2 km+4\alpha^2 b^2}}{2\alpha m}t} \tag{4.26}$$

$$\Delta x_2 = v_0 + C_4 e^{-\frac{1}{\alpha m}t} + C_2 e^{\frac{-1-2\alpha b-\sqrt{1-8\alpha^2 km+4\alpha^2 b^2}}{2\alpha m}t} + C_3 e^{\frac{-1-2\alpha b+\sqrt{1-8\alpha^2 km+4\alpha^2 b^2}}{2\alpha m}t} \tag{4.27}$$

Finally, change in distance between the two particles can be expressed as the difference of calculated positional perturbations.

$$|\Delta x_1 - \Delta x_2| = \left| 2C_2 e^{\frac{-1-2\alpha b-\sqrt{1-8\alpha^2 km+4\alpha^2 b^2}}{2\alpha m}t} + 2C_3 e^{\frac{-1-2\alpha b+\sqrt{1-8\alpha^2 km+4\alpha^2 b^2}}{2\alpha m}t} \right| \tag{4.28}$$

Here, we see that the inclusion of anticipation makes $|\Delta x_1 - \Delta x_2|$ decay faster to its steady-state value due to additional $-2\alpha b$ related terms in the exponents. Hence, anticipation introduces yet another control parameter again, along with the spatial mass.

4.3 Two-Particle AE Models: Side-by-Side Configuration

The configuration for side-by-side two-particle AE model with symmetrical boundary condition is given below.

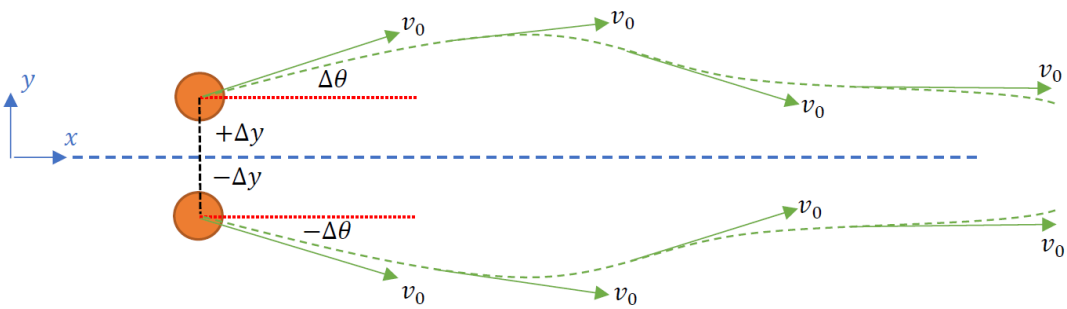

Figure 4.2: Side-by-Side Configuration for Two-Particle AE

Different from the head-to-tail one, side-by-side configuration introduces rotational freedoms of the agents.

4.3.1 Side-by-Side in 1st Order w/o Anticipation

Over-damped equations of motion are constructed below.

$$\Delta\dot{v} = v_0 - \alpha k 2\Delta y \sin\Delta\theta \tag{4.29}$$

$$\Delta\dot{\theta} = -\beta k 2\Delta y \cos\Delta\theta \tag{4.30}$$

Equations are to be extended component-wise.

$$\Delta\dot{x} = v_0 \cos\Delta\theta - \alpha k 2\Delta y \sin\Delta\theta \cos\Delta\theta \tag{4.31}$$

$$\Delta\dot{y} = v_0 \sin\Delta\theta - \alpha k 2\Delta y \sin^2\Delta\theta \tag{4.32}$$

$$\Delta\dot{\theta} = -\beta k 2\Delta y \cos\Delta\theta \tag{4.33}$$

With small-angle-approximation, equations of motions are linearized.

$$\Delta\dot{x} = v_0 - \alpha k 2\Delta y \Delta\theta \tag{4.34}$$

$$\Delta\dot{y} = v_0 \Delta\theta \tag{4.35}$$

$$\Delta\dot{\theta} = -\beta k 2\Delta y \tag{4.36}$$

Then, the model in only first-order terms becomes a system of ODEs.

$$\begin{Bmatrix} \Delta\dot{y} \\ \Delta\dot{\theta} \end{Bmatrix} = \begin{bmatrix} 0 & v_0 \\ -2\beta k & 0 \end{bmatrix} \begin{Bmatrix} \Delta y \\ \Delta\theta \end{Bmatrix} \tag{4.37}$$

For stability analysis, eigenvalues of our system matrix are to be calculated.

$$\text{eig} \begin{pmatrix} 0 & v_0 \\ -2\beta k & 0 \end{pmatrix} \rightarrow \boxed{\lambda_- = -\sqrt{-2\beta k v_0}, \quad \lambda_+ = \sqrt{-2\beta k v_0}} \tag{4.38}$$

Eigenvalues reflect pure oscillations regardless of the parameter selection since real parts are always zero.

Analytical solutions for positional/rotational perturbations can be easily expressed using above-calculated eigenvalues.

$$\Delta y = C_1 e^{-\sqrt{-2\beta k v_0} t} + C_2 e^{\sqrt{-2\beta k v_0} t} \tag{4.39}$$

$$\Delta\theta = \frac{\beta k l + C_1 \lambda_+ e^{\lambda_- t} + C_2 \lambda_- e^{\lambda_+ t}}{2\beta k} \tag{4.40}$$

Finally, change in distance between the two particles can be expressed directly as $|2\Delta y(t)|$.

$$|2\Delta y| = |2C_1 e^{-\sqrt{-2\beta k v_0} t} + 2C_2 e^{\sqrt{-2\beta k v_0} t}| \tag{4.41}$$

4.3.2 Side-by-Side in 1st Order w/ Anticipation

Over-damped equations of motion are constructed below.

$$\Delta\dot{v} = v_0 - \alpha[k 2\Delta y + b 2\Delta\dot{y}] \sin\Delta\theta \tag{4.42}$$

$$\Delta\dot{\theta} = -\beta[k 2\Delta y + b 2\Delta\dot{y}] \cos\Delta\theta \tag{4.43}$$

Equations are to be extended component-wise.

$$\Delta\dot{x} = v_0 \cos\Delta\theta - \alpha[k2\Delta y + b2\Delta\dot{y}]\sin\Delta\theta\cos\Delta\theta \tag{4.44}$$

$$\Delta\dot{y} = v_0 \sin\Delta\theta - \alpha[k2\Delta y + b2\Delta\dot{y}]\sin^2\Delta\theta \tag{4.45}$$

$$\Delta\dot{\theta} = -\beta[k2\Delta y + b2\Delta\dot{y}]\cos\Delta\theta \tag{4.46}$$

With small-angle-approximation, equations of motions are linearized.

$$\Delta\dot{x} = v_0 - \alpha[k2\Delta y + b2\Delta\dot{y}]\Delta\theta \tag{4.47}$$

$$\Delta\dot{y} = v_0\Delta\theta \tag{4.48}$$

$$\Delta\dot{\theta} = -\beta[k2\Delta y + b2\Delta\dot{y}] \tag{4.49}$$

Then, the model in only first-order terms becomes a system of ODEs.

$$\begin{Bmatrix} \Delta\dot{y} \\ \Delta\dot{\theta} \end{Bmatrix} = \begin{bmatrix} 0 & v_0 \\ -2\beta k & -2\beta b v_0 \end{bmatrix} \begin{Bmatrix} \Delta y \\ \Delta\theta \end{Bmatrix} \tag{4.50}$$

For stability analysis, eigenvalues of our system matrix are to be calculated.

$$\text{eig}\begin{pmatrix} 0 & v_0 \\ -2\beta k & -2\beta b v_0 \end{pmatrix} \rightarrow \boxed{\lambda_\pm = -\beta b v_0 \pm \sqrt{\beta^2 b^2 v_0^2 - 2\beta k v_0}} \tag{4.51}$$

For $v_0 < \beta b^2/(2k)$, both eigenvalues are real & negative and any oscillation is over-damped. For $v_0 > \beta b^2/(2k)$, negative real parts are accompanied by imaginary parts, so it is expected to see some damped oscillations as the system reaches its aligned state. Hence, anticipation in this scenario behaves similar to damping as an additional control parameter introducing negative real parts.

Analytical solutions for positional/rotational perturbations can be easily expressed using above-calculated eigenvalues.

$$\Delta y = C_1 e^{\left(-\beta b v_0 - \sqrt{\beta^2 b^2 v_0^2 - 2\beta k v_0}\right)t} + C_2 e^{\left(-\beta b v_0 + \sqrt{\beta^2 b^2 v_0^2 - 2\beta k v_0}\right)t} \tag{4.52}$$

$$\Delta\theta = \frac{\beta k l + C_1\lambda_+ e^{\lambda_- t} + C_2\lambda_- e^{\lambda_+ t}}{2\beta k} \tag{4.53}$$

Finally, change in distance between the two particles can be expressed directly as $|2\Delta y(t)|$.

$$|2\Delta y| = \left| 2C_1 e^{\left(-\beta b v_0 - \sqrt{\beta^2 b^2 v_0^2 - 2\beta k v_0}\right)t} + 2C_2 e^{\left(-\beta b v_0 + \sqrt{\beta^2 b^2 v_0^2 - 2\beta k v_0}\right)t} \right| \tag{4.54}$$

4.3.3 Side-by-Side in 2nd Order w/o Anticipation

Over-damped equations of motion are constructed below.

$$\alpha m \Delta \ddot{v} + \Delta \dot{v} = v_0 - \alpha k 2 \Delta y \sin \Delta\theta \tag{4.55}$$

$$\beta I \Delta \ddot{\theta} + \Delta \dot{\theta} = -\beta k 2 \Delta y \cos \Delta\theta \tag{4.56}$$

Equations are to be extended component-wise.

$$\alpha m \Delta \ddot{x} + \Delta \dot{x} = v_0 \cos \Delta\theta - \alpha k 2 \Delta y \sin \Delta\theta \cos \Delta\theta \tag{4.57}$$

$$\alpha m \Delta \ddot{y} + \Delta \dot{y} = v_0 \sin \Delta\theta - \alpha k 2 \Delta y \sin^2 \Delta\theta \tag{4.58}$$

$$\beta I \Delta \ddot{\theta} + \Delta \dot{\theta} = -\beta k 2 \Delta y \cos \Delta\theta \tag{4.59}$$

With small-angle-approximation, equations of motions are linearized.

$$\alpha m \Delta \ddot{x} + \Delta \dot{x} = v_0 - \alpha k 2 \Delta y \Delta\theta \tag{4.60}$$

$$\alpha m \Delta \ddot{y} + \Delta \dot{y} = v_0 \Delta\theta \tag{4.61}$$

$$\beta I \Delta \ddot{\theta} + \Delta \dot{\theta} = -\beta k 2 \Delta y \tag{4.62}$$

Introducing $\Delta \dot{y} = \Delta u$ and $\Delta \dot{\theta} = \Delta w$, the model in only first-order terms becomes a system of ODEs.

$$\begin{Bmatrix} \Delta \dot{y} \\ \Delta \dot{\theta} \\ \Delta \dot{u} \\ \Delta \dot{w} \end{Bmatrix} = \begin{bmatrix} 0 & 0 & 1 & 0 \\ 0 & 0 & 0 & 1 \\ 0 & \frac{v_0}{\alpha m} & -\frac{1}{\alpha m} & 0 \\ -\frac{2k}{I} & 0 & 0 & -\frac{1}{\beta I} \end{bmatrix} \begin{Bmatrix} \Delta y \\ \Delta \theta \\ \Delta u \\ \Delta w \end{Bmatrix} \tag{4.63}$$

For stability analysis, eigenvalues of our system matrix are to be calculated.

$$\begin{aligned} &\begin{vmatrix} -\lambda & 0 & 1 & 0 \\ 0 & -\lambda & 0 & 1 \\ 0 & \frac{v_0}{\alpha m} & -\frac{1}{\alpha m} - \lambda & 0 \\ -\frac{2k}{I} & 0 & 0 & -\frac{1}{\beta I} - \lambda \end{vmatrix} \\ &= -\lambda \left\{ -\lambda \left[\left(-\frac{1}{\alpha m} - \lambda \right) \left(-\frac{1}{\beta I} - \lambda \right) \right] \right\} + \frac{2k}{I} \frac{v_0}{\alpha m} \\ &= \left[\left(\frac{1}{\alpha m} + \lambda \right) \left(\frac{1}{\beta I} + \lambda \right) \right] \lambda^2 + \frac{2k}{I} \frac{v_0}{\alpha m} \\ &= \left(\lambda^2 + \frac{\beta I + \alpha m}{\beta I \alpha m} \lambda + \frac{1}{\beta I \alpha m} \right) \lambda^2 + \frac{2k}{I} \frac{v_0}{\alpha m} \\ &= \lambda^4 + \frac{\beta I + \alpha m}{\beta I \alpha m} \lambda^3 + \frac{1}{\beta I \alpha m} \lambda^2 + \frac{2k v_0}{I \alpha m} \end{aligned} \tag{4.64}$$

Eqn.(4.64) can be converted to a *depressed quartic equation* using Lodovico Ferrari's solution, which requires an exhaustive set of calculation steps. It is still valuable to see that additional angular DOF from side-by-side configuration yields new control parameters β and I, namely inverse rotational damping coefficient and rotational inertia, in addition to all parameters from head-to-tail configuration.

4.3.4 Side-by-Side in 2nd Order w/ Anticipation

Over-damped equations of motion are constructed below.

$$\alpha m \Delta\ddot{v} + \Delta\dot{v} = v_0 - \alpha[k2\Delta y + b2\Delta\dot{y}]\sin\Delta\theta \tag{4.65}$$

$$\beta I \Delta\ddot{\theta} + \Delta\dot{\theta} = -\beta[k2\Delta y + b2\Delta\dot{y}]\cos\Delta\theta \tag{4.66}$$

Equations are to be extended component-wise.

$$\alpha m \Delta\ddot{x} + \Delta\dot{x} = v_0\cos\Delta\theta - \alpha[k2\Delta y + b2\Delta\dot{y}]\sin\Delta\theta\cos\Delta\theta \tag{4.67}$$

$$\alpha m \Delta\ddot{y} + \Delta\dot{y} = v_0\sin\Delta\theta - \alpha[k2\Delta y + b2\Delta\dot{y}]\sin^2\Delta\theta \tag{4.68}$$

$$\beta I \Delta\ddot{\theta} + \Delta\dot{\theta} = -\beta[k2\Delta y + b2\Delta\dot{y}]\cos\Delta\theta \tag{4.69}$$

With small-angle-approximation, equations of motions are linearized.

$$\alpha m \Delta\ddot{x} + \Delta\dot{x} = v_0 - \alpha[k2\Delta y + b2\Delta\dot{y}]\Delta\theta \tag{4.70}$$

$$\alpha m \Delta\ddot{y} + \Delta\dot{y} = v_0\Delta\theta \tag{4.71}$$

$$\beta I \Delta\ddot{\theta} + \Delta\dot{\theta} = -\beta[k2\Delta y + b2\Delta\dot{y}] \tag{4.72}$$

Introducing $\Delta\dot{y} = \Delta u$ and $\Delta\dot{\theta} = \Delta w$, the model in only first-order terms becomes a system of ODEs.

$$\begin{Bmatrix} \Delta\dot{y} \\ \Delta\dot{\theta} \\ \Delta\dot{u} \\ \Delta\dot{w} \end{Bmatrix} = \begin{bmatrix} 0 & 0 & 1 & 0 \\ 0 & 0 & 0 & 1 \\ 0 & \frac{v_0}{\alpha m} & -\frac{1}{\alpha m} & 0 \\ -\frac{2k}{I} & 0 & -\frac{2b}{I} & -\frac{1}{\beta I} \end{bmatrix} \begin{Bmatrix} \Delta y \\ \Delta\theta \\ \Delta u \\ \Delta w \end{Bmatrix} \tag{4.73}$$

For stability analysis, eigenvalues of our system matrix are to be calculated.

$$
\begin{aligned}
&\begin{vmatrix} -\lambda & 0 & 1 & 0 \\ 0 & -\lambda & 0 & 1 \\ 0 & \frac{v_0}{\alpha m} & -\frac{1}{\alpha m} - \lambda & 0 \\ -\frac{2k}{I} & 0 & -\frac{2b}{I} & -\frac{1}{\beta I} - \lambda \end{vmatrix} \\
&= -\lambda \left\{ -\lambda \left[\left(-\frac{1}{\alpha m} - \lambda \right) \left(-\frac{1}{\beta I} - \lambda \right) \right] - \frac{2b}{I} \frac{v_0}{\alpha m} \right\} + \frac{2k}{I} \frac{v_0}{\alpha m} \\
&= \left[\left(\frac{1}{\alpha m} + \lambda \right) \left(\frac{1}{\beta I} + \lambda \right) \right] \lambda^2 + \frac{2b}{I} \frac{v_0}{\alpha m} \lambda + \frac{2k}{I} \frac{v_0}{\alpha m} \\
&= \left(\lambda^2 + \frac{\beta I + \alpha m}{\beta I \alpha m} \lambda + \frac{1}{\beta I \alpha m} \right) \lambda^2 + \frac{2b}{I} \frac{v_0}{\alpha m} \lambda + \frac{2k}{I} \frac{v_0}{\alpha m} \\
&= \lambda^4 + \frac{\beta I + \alpha m}{\beta I \alpha m} \lambda^3 + \frac{1}{\beta I \alpha m} \lambda^2 + \frac{2 b v_0}{I \alpha m} \lambda + \frac{2 k v_0}{I \alpha m}
\end{aligned}
\tag{4.74}
$$

Again, Eqn.(4.74) can be converted to a *depressed quartic equation* using Lodovico Ferrari's solution, which requires an exhaustive set of calculation steps. Anticipation introduces a new control parameter on top of all the previous ones, which is very similar to that of head-to-tail configurations with anticipation.

CHAPTER 5

NUMERICAL EXPERIMENTS

5.1 Performance Metrics

Extending the previous type of analysis from Chapter 4 to systems with more than two agents requires performance metrics so as to evaluate differences between two-particle analysis and numerical multi-agent simulations. In order to subject toy models to test in terms of emergent properties, the most sound parameter candidates are the eigenvalues. For a valid comparison, an equivalent definition needs to be extracted from larger systems as an eigenvalue substitute. Considering that real and imaginary parts of the toy model eigenvalues are related to damping ratios and response frequencies, respectively; similar corresponding kinematic values can be inferred from multi-agent simulations. Looking for an overall damping ratio correlation makes more sense since it is expected to have different frequency responses per various system sizes. When an ensemble of agents move through space, the obvious oscillations always occur in their heading angles. Therefore, multi-agent damping ratios are selected to be extracted from the decaying angular oscillation waves by simply fitting an enveloping exponential curve.

The second metric for performance measures is the distance between agents. Tracing minimum, maximum and average distances for each time-step over the whole run-time yields how much responsive agents are. If the minimum distance is larger in one run compared to the other, one with the larger minimum distance is assumed to be more responsive since agents outspeed avoiding each other. Similar claim is valid for the opposite case in which smaller maximum distance assumes more responsive repulsion forces so that agents do not favour disassembling. The caveat of such a

faster response is the reduction in system speed after a critical point, which is in analogy with excessively pre-cautious and observant agents.

Looking from a swarm engineering perspective, the very last but not least parameters prone to tuning are anticipation and inertia. In order to assess the performance of each parameter, a metric is to be introduced for the sole evaluation purpose of controlled experiments. It is common in AE model studies that the region order-disorder transition occurs plays an important role by means of how these parameters affect the system performance [1, 2, 25–27, 47]. These transitions are defined when agents' degree of alignment changes drastically. The metric for such information in AM systems is called the usual *polarization* order parameter which is defined as below.

$$\psi = \frac{1}{N} \left\| \sum_{i=1}^{N} \hat{n}_i \right\| \tag{5.1}$$

$\psi = 1$ when all agents are perfectly aligned. On the other hand, $\psi = 0$ means all the agents have random orientations. It is expected to have a decrease in *polarization* once actuation noise strength coefficient D_θ surpasses a certain threshold, namely the transition region. Effects of anticipation and inertia on the position of such transition points are to be investigated. The relation between anticipation and transition point would reveal in what trend to tune control algorithms by means of anticipation parameter for a better swarm robotics robustness. Similarly, the relation between inertia and transition region would determine which of lightweight or heavy designs to favour for less noise susceptibility.

5.2 Experimental Setups

It is essential to emphasize different measures of performance metrics from Section 5.1 by cleverly built experimental setups. Required reasoning scale ranges from how to configure individual units up to setting environmental conditions. To start with, agents are to be located in a hexagonal formation with triangular lattices, which is one of the AM configurations common in AE models. They all have self-propulsion velocities with both ordered or random initial states in terms of their heading directions. Agents are assumed to be two-wheeled robots so that lateral translations are restricted, just as how AE models define movements only in translations along their

heading directions and rotations about their own axes. This restriction is actually intrinsic to equations of motion for all AE models so that forces projecting to heading direction creates spatial movements, whereas the other perpendicular components result in rotations.

Apart from the agent topology, environmental conditions are also designed to vary for different setups. The main simplistic variances in swarm environments are generally existence and allocation of the obstacles. For this purpose, two obstacle layouts are to be introduced so that agents are kinetically related once they are within a vicinity close enough to trigger sensors. These layouts are selected as ducts and walls whose kinetics are modelled as circles/cylinders with finite and infinite radii, respectively. It is to be shown that different anticipation values change the way ensemble handles obstacles. For instance, existence of anticipation can enable duct passage rather then being reflected from the circles/cylinders once parameters are tuned correctly. A similar effect is acquirable regarding how they bounce from the wall.

5.3 Multi-Agent Simulator

Experimental setups described in Section 5.2 are to be numerically implemented by realization of a multi-agent simulator which is scripted using commercially available software package MATLAB. Numerical and boolean parameters utilized as an input for the simulator are tabulated in Tables 5.1 and 5.2 with their typical order-of-magnitudes/states below. Figures 5.1a and 5.1b demonstrate enabled ducts and walls, separately.

In addition to pre-defined arena sizes, a periodic boundary condition is implemented at the borders through which agents are teleported to the other facing edge once they pass. This effect simultaneously works along both horizontal and vertical limits (see Figures 5.2a and 5.2b).

As stated in Section 3.4, it is trivial to add proportional velocity controller so as to include inertial effects. Hence, both spatial and rotational inertias are introduced to the multi-agent simulator as dynamic relaxations for wider parameter ranges with stable behaviours. Inertial effects are enabled in the first place by uncommenting the

related equations of motion lines.

Yet another aspect of the multi-agent simulator is parallelization specifically for order-disorder transition studies. When such curves are achieved, each and every point on the curve data corresponds to a single run of simulation. Therefore, time required for simulations is drastically reduced by making use of multi-threading.

Table 5.1: Numerical Inputs Used in Multi-Agent Simulator

Parameter	Name	Description	Typical Values
Time increment	dt	Resolution for the simulation	$0.01 - 0.1$
Final time	t_f	Simulation duration	$1e4 - 1e6$
Self-propulsion	v_0	Forward biasing speed	$0.001 - 0.005$
Damping	alpha	Inverse translational damp. coeff.	$0.001 - 0.005$
Damping	beta	Inverse rotational damp. coeff.	$0.05 - 0.2$
Spring constant	K	Free length of unity	$1 - 25$
Anticipation	b	AEAnt to AES when zero	$0 - 75$
Arena size	x_BC	Horizontal length of the arena	$[-5\ 5] - [-50\ 50]$
Arena size	y_BC	Vertical length of the arena	$[-5\ 5] - [-50\ 50]$
Shell	shell	Radius of the voronoi shell	$1 - 2$
Duct position	obs_X	X-position of the ducts	within x_BC
Duct position	obs_Y	Y-position of the ducts	within y_BC
Duct radius	obs_R	Radius of the duct circles	$1 - 10$
Duct forcing	obs_K	Force gain	$0.1 - 2.5$
Duct interaction	obs_off	Interaction offset from the duct	$0 - 2$
Wall position	bnc_X	X-position of the wall	within x_BC
Wall forcing	bnc_K	Force gain	$0.1 - 2.5$
Wall interaction	bnc_off	Interaction offset from the wall	$0 - 2$
Noise	D_r	Sensing noise coefficient	$1e - 8 - 1e - 6$
Noise	D_theta	Actuation noise coefficient	$1e - 8 - 1e - 6$
Ensemble size	L	Side length of the hexagon placement	$3 - 10$
Initial randomness	D_pert	Initial angular perturbation coefficient	$0 - \pi$

Table 5.2: Boolean Inputs Used in Multi-Agent Simulator

Parameter	Name	Description	Typical States
Anticipation	anticipation	Sets b to the assigned value	$false - true$
Dynamic Network	dynamicNetwork	Dynamic linking within shell	$false - true$
Ducts	obstacle	Puts circular ducts	$false - true$
Wall	bounce	Puts a bouncing wall	$false - true$
Noise	noise	Enables sensing/actuation noise	$false - true$
Initial randomness	perturbation	Enables initial angular perturbation	$false - true$

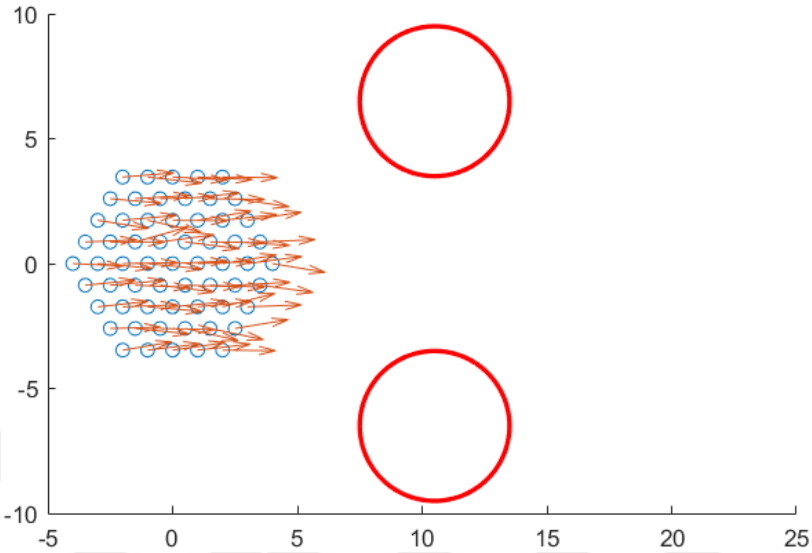

(a) Ducts

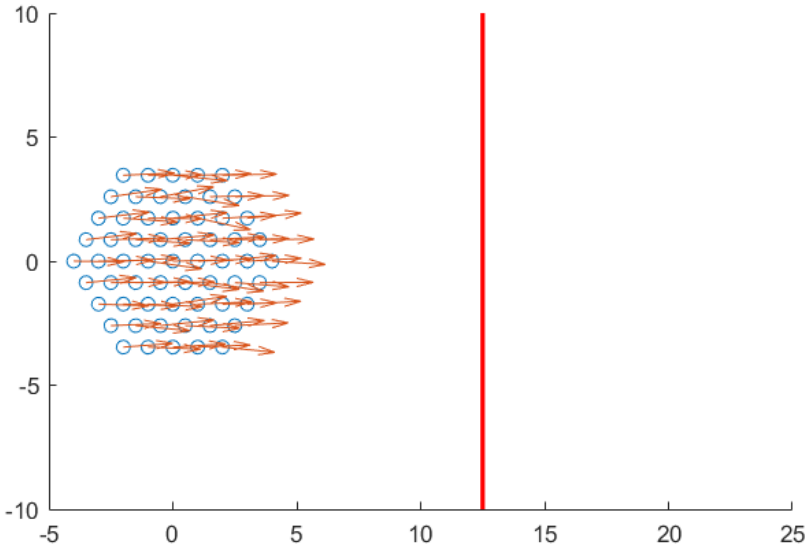

(b) Wall

Figure 5.1: Enabled Circular Ducts and Wall

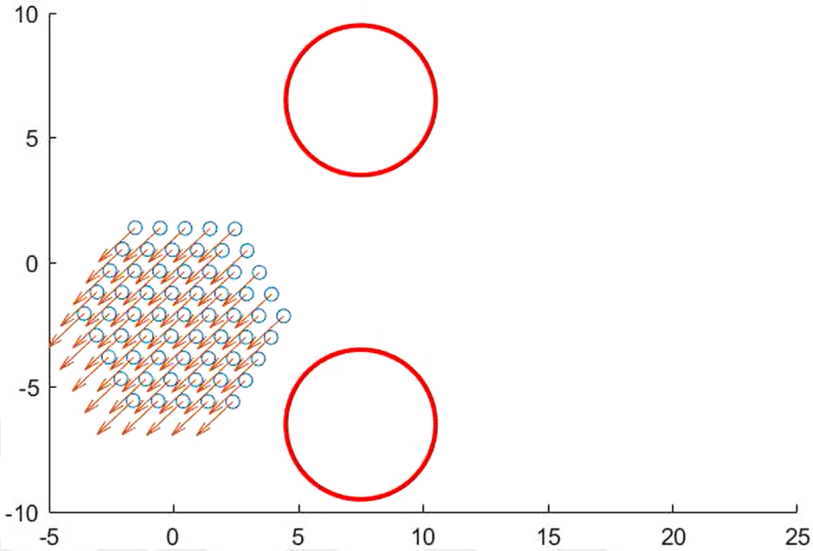

(a) Before Crossing

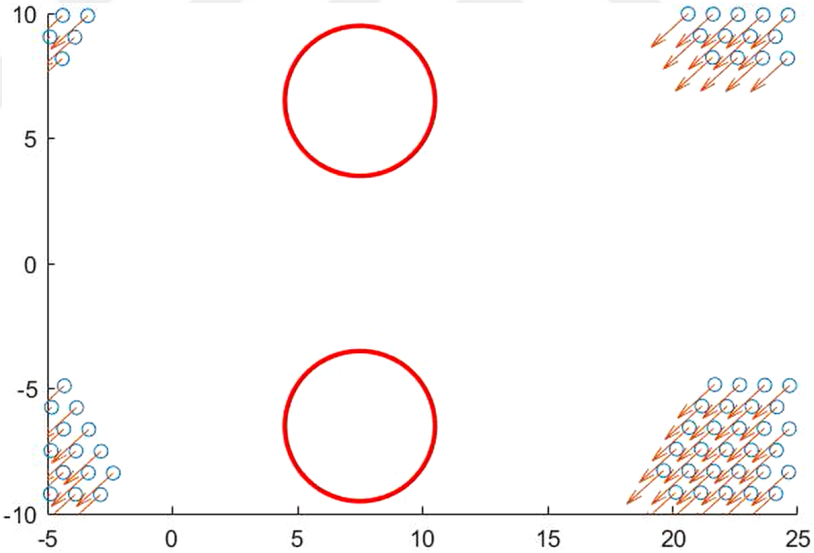

(b) After Crossing

Figure 5.2: Demonstration of Periodic Boundary Conditions

CHAPTER 6

RESULTS & DISCUSSION

6.1 Similarities between AEA and AEAnt

Active Elastic Alignment (AEA) and Active Elastic Anticipation (AEAnt) are fundamentally two particular models with distinctive configurations. On the other hand, they have similar mathematical definitions with different parameters. Lin et al. [2] formulates their system with Eq. (3.14) under small perturbations. Yet similar linearized system of equations in Eq. (4.50) is derived for side-by-side 1st order toy model configuration with anticipation (see Section 4.3.2). They are listed below for a better comparison.

Table 6.1: System of Linearized Equations for AEA vs. AEAnt

Model	System of Linearized Equations
Active Elastic Alignment (AEA)	$\begin{Bmatrix} \Delta\dot{r} \\ \Delta\dot{\phi} \end{Bmatrix} = \begin{bmatrix} 0 & v_0 \\ -2\beta k & -2\beta k R \end{bmatrix} \begin{Bmatrix} \Delta r \\ \Delta\phi \end{Bmatrix}$
Active Elastic Anticipation (AEAnt)	$\begin{Bmatrix} \Delta\dot{y} \\ \Delta\dot{\theta} \end{Bmatrix} = \begin{bmatrix} 0 & v_0 \\ -2\beta k & -2\beta b v_0 \end{bmatrix} \begin{Bmatrix} \Delta y \\ \Delta\theta \end{Bmatrix}$

It is trivial to see that AEA and AEAnt have common mathematical expressions by means of different parameter representations such that $bv_0 \equiv kR$. An analogy between two definitions can be constructed such that extrapolating future position of a neighbour is equivalent to applying spring forces at that instant with an offset as if the agent is at that anticipated point. In summary, AEAnt predicts the future, yet AEA already applies kinetics in advance from that anticipated position.

6.2 Eigenvalue Plots for Toy Models

In this section, eigenvalue plots for each analytical models from Chapter 4 are given. Changes in eigenvalues as a function of both anticipation and inertial parameters are plotted so that stability analysis can be performed. Typical values from Tables 5.1 and 5.2 are assigned for numerical representations.

The very first observation in both eigenvalue expressions and plots is that head-to-tail configuration is always non-oscillatory with negative real eigenvalues (see Figures 6.1 and 6.2). On the other hand, side-by-side configuration introduces damped oscillations in both 1st and 2nd orders due to additional angular DOFs (see Figure 6.3 for 1st order and Figures 6.4, 6.5, 6.6 for 2nd order).

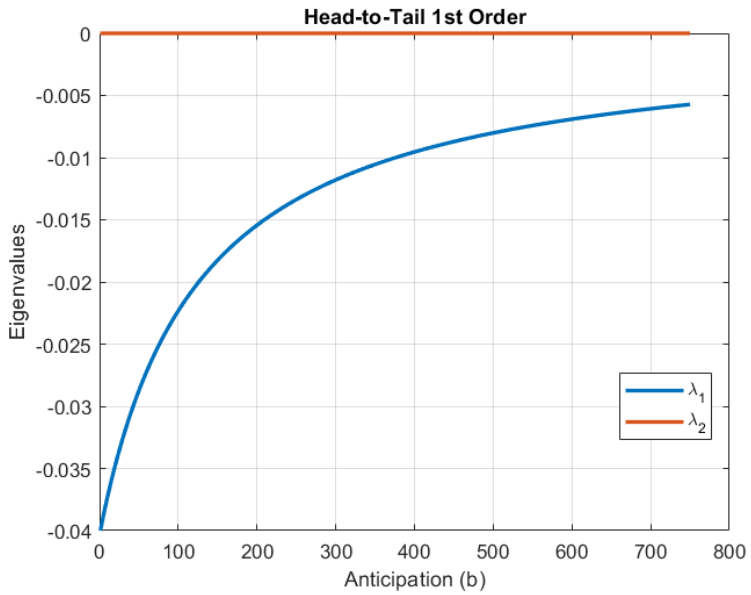

(a) Plot of $\lambda_i(b)$ from Eqn. (4.11) for Head-to-Tail Configuration in 1st Order

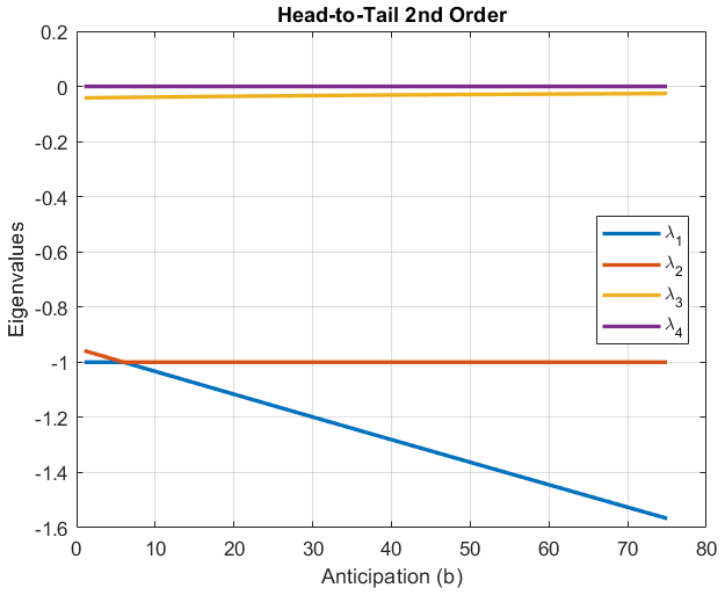

(b) Plot of $\lambda_i(b)$ from Eqn. (4.25) for Head-to-Tail Configuration in 2nd Order

Figure 6.1: Eigenvalue Plots as a Function of Anticipation for Head-to-Tail Configuration in both 1st and 2nd Orders

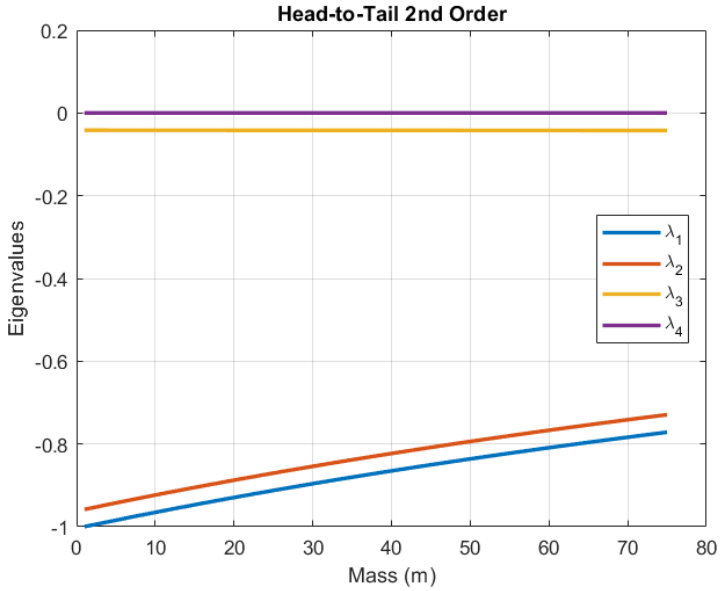

Figure 6.2: Plot of $\lambda_i(m)$ from Eqn. (4.25) for Head-to-Tail Configuration in 2nd Order

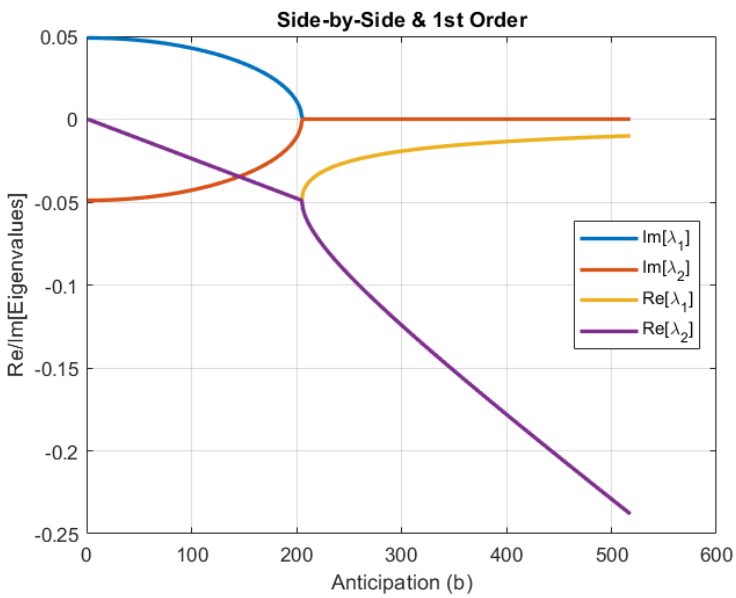

Figure 6.3: Plot of $\lambda_i(b)$ from Eqn. (4.51) for Side-by-Side Configuration in 1st Order

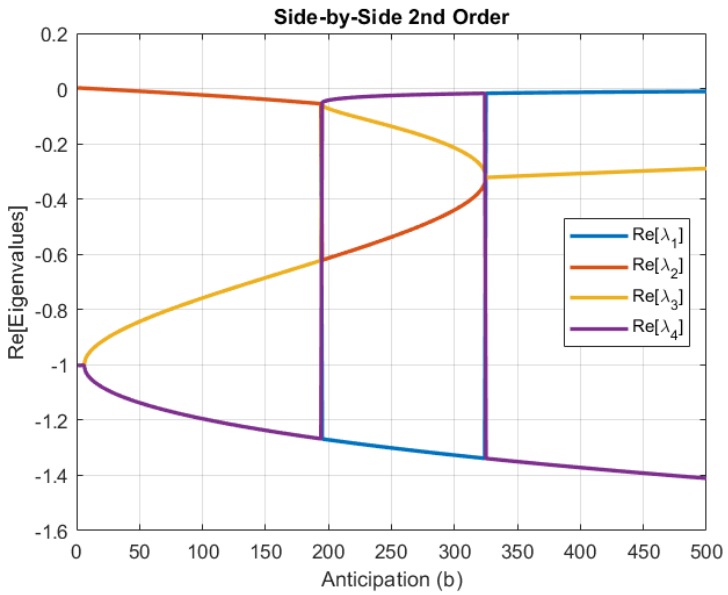

(a) Plot of Re[$\lambda_i(b)$] from Eqn. (4.74) for Side-by-Side Configuration in 2nd Order

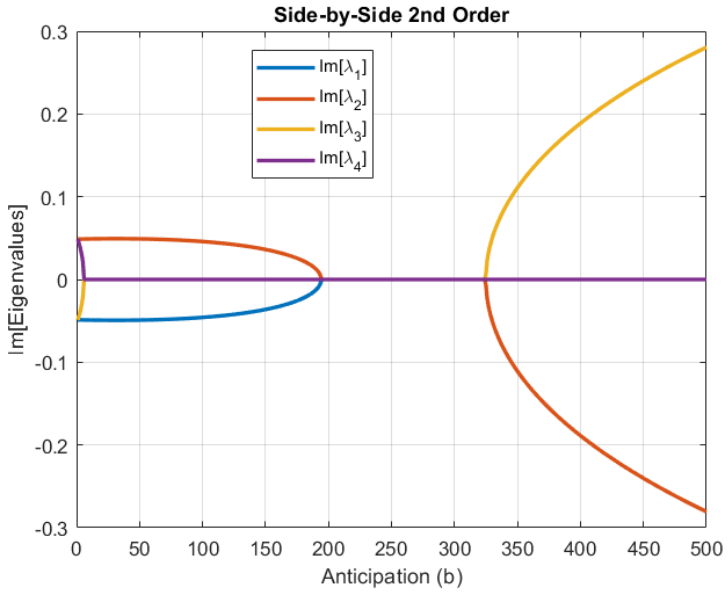

(b) Plot of Im[$\lambda_i(b)$] from Eqn. (4.74) for Side-by-Side Configuration in 2nd Order

Figure 6.4: Eigenvalue Plots as a Function of Anticipation for Side-by-Side Configuration in 2nd Order

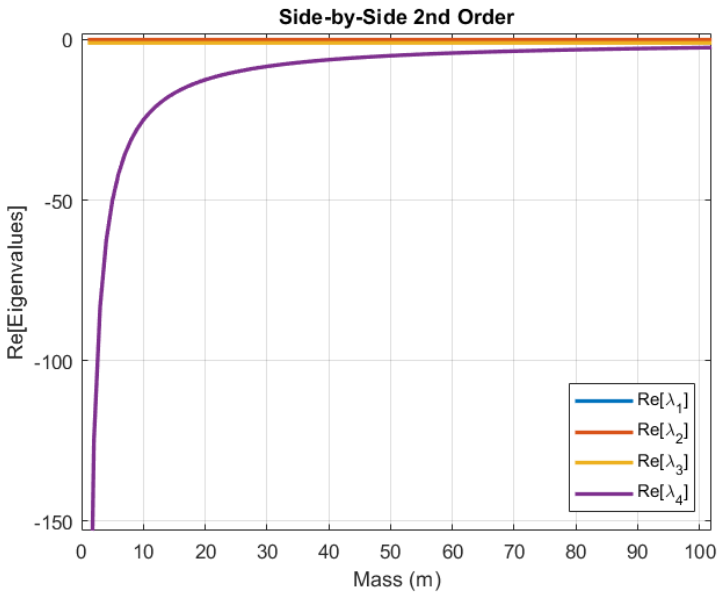

(a) Plot of Re[$\lambda_i(m)$] from Eqn. (4.74) for Side-by-Side Configuration in 2nd Order

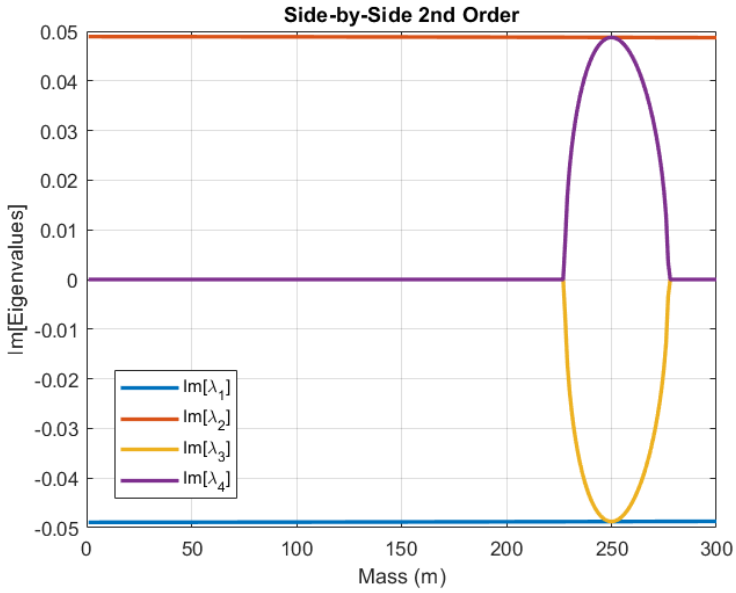

(b) Plot of Im[$\lambda_i(m)$] from Eqn. (4.74) for Side-by-Side Configuration in 2nd Order

Figure 6.5: Eigenvalue Plots as a Function of Mass for Side-by-Side Configuration in 2nd Order

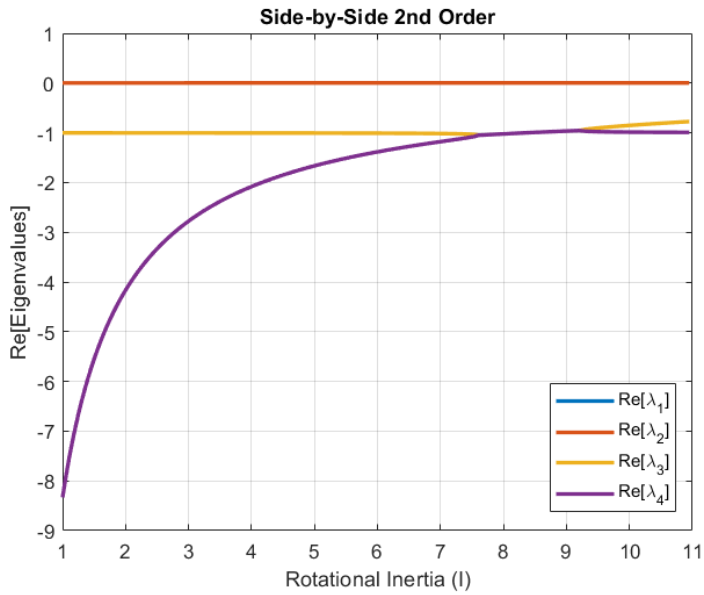

(a) Plot of Re[$\lambda_i(I)$] from Eqn. (4.74) for Side-by-Side Configuration in 2nd Order

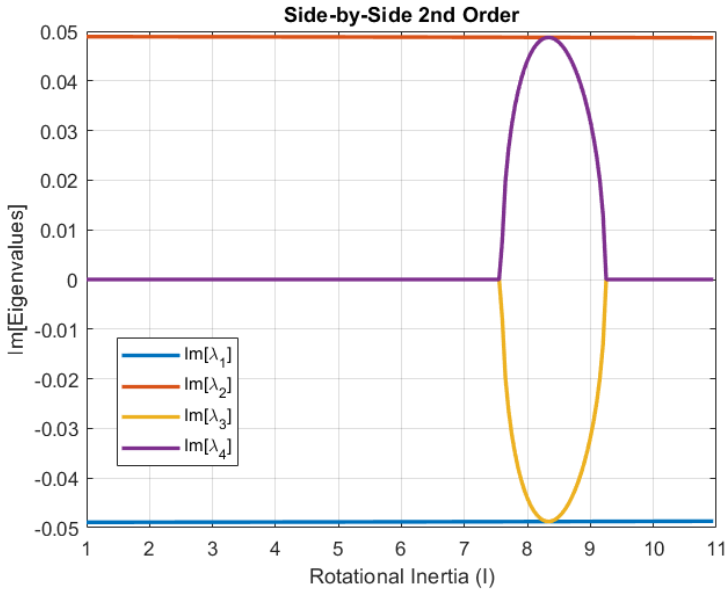

(b) Plot of Im[$\lambda_i(I)$] from Eqn. (4.74) for Side-by-Side Configuration in 2nd Order

Figure 6.6: Eigenvalue Plots as a Function of Rotational Inertia for Side-by-Side Configuration in 2nd Order

6.3 Toy Models vs. Multi-Agent Simulator

Toy models and results from multi-agent simulations are to be compared both quantitatively and qualitatively as one of the main objectives of this thesis. Given the analytical models of two-particle AE systems, only side-by-side configuration results in oscillations as how it is commonly expected and observed in multi-agent systems. Eigenvalues of the analytical models are compared to the parameters measured from multi-agent systems for the purpose of assessing extrapolation characteristics. In order to be consistent with pure analytical approach and Lin et al. [2], only 1st order systems are investigated as a function of anticipation parameter. 2nd order expressions are to be used for inertial effect comparisons later this chapter. To start with, real and imaginary parts of the eigenvalues for two-particle AE in side-by-side configuration are plotted as a function of anticipation parameter at Figure 6.3.

It is observed that there exists a critical value of anticipation for which imaginary parts of the eigenvalues diminish and leave the system with over-damping from that point on. This seems to be analogous with harmonic oscillator whose oscillations are critically damped for a certain value of damping ratio. In terms of control engineering perspective, existence of such a point promises broad range of characteristics depending on performance requirements. How responsive a swarm is to behave can be tuned given the condition that multi-agent systems have the same pattern. Real and imaginary parts of the eigenvalues are to be decoupled for separate investigations in order to discover such oscillation and damping characteristics.

Considering the size of multi-agent systems, expecting their frequency responses to be in correlation with toy models is not practical as information travelling through agents results in a kinematic inertia. Therefore, real parts of the eigenvalues are to be examined as a reflection to damping behaviour of multi-agent systems. If the orientation angles of each and every agents are plotted as a function of time, systems with anticipation results in gradual decrease by means of oscillation amplitudes. This effect can be seen at Figure 6.7 below.

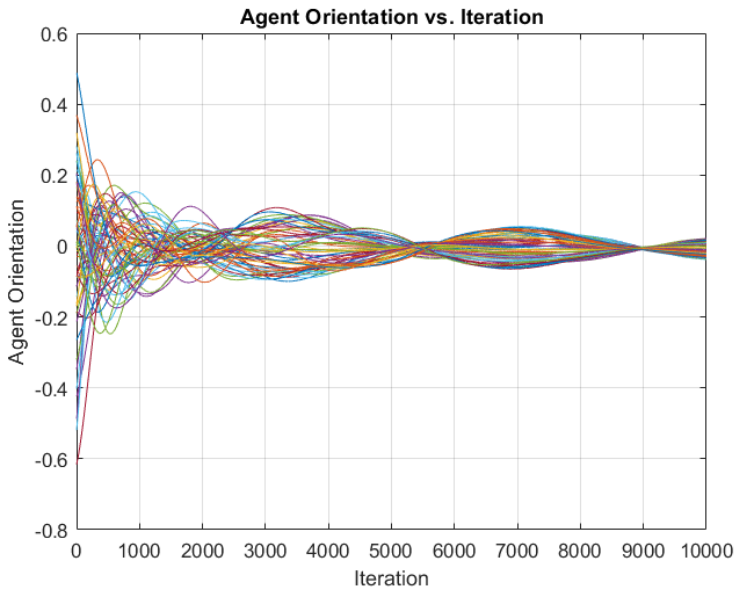

Figure 6.7: Agent Orientation vs. Time in a Multi-Agent System w/ Anticipation

It is obvious that one can easily fit an exponential decay envelope to these curves, and extract damping ratios for different runs with changing anticipation values given that all other parameters are fixed. With a certain precision of anticipation range, a damping ratio curve as a function of anticipation is achieved and one example of a comparison plot with the real parts of analytical eigenvalues are given below at Figure 6.8.

It is valuable to see that the linear decreasing trends are common in both of the systems despite their different slopes and scales. It promises that a particular set of tuned parameters might result in the same damping ratios with the toy model. Not only the common trends are existent but also a critical anticipation point may exist as in the case of toy model eigenvalues. Existence of such critical anticipation value is worthwhile to be discovered as it carries a great potential for swarm robotics applications by means of a control parameter. Investigation of critical anticipation has its own challenges as numerical instabilities become the restricting factor and it is left to be discussed as a future work.

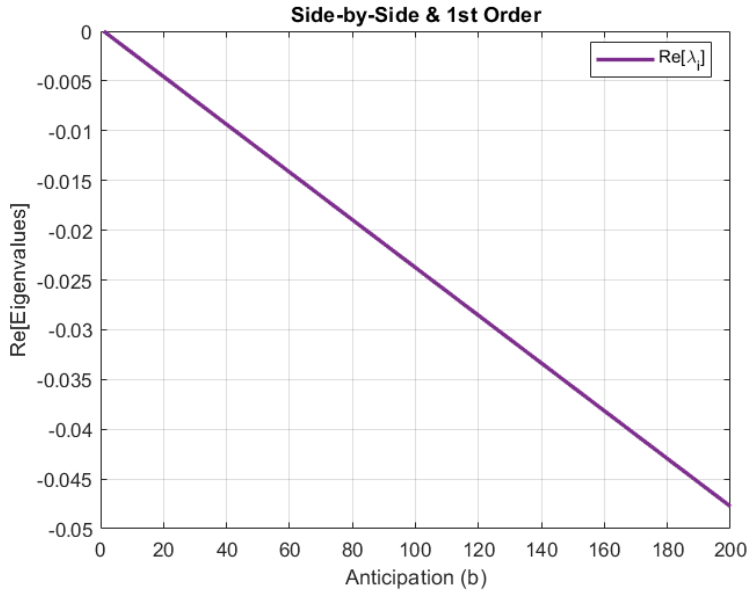

(a) Plot of Re[$\lambda_i(b)$] from Eqn. (4.51) for Side-by-Side Configuration in 1st Order

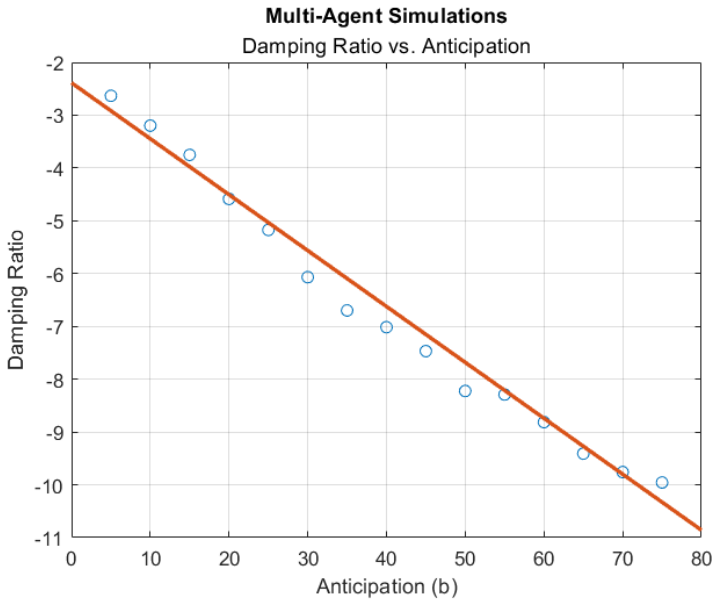

(b) Damping Ratios Extracted from Multi-Agent Simulations w/ Typical Values

Figure 6.8: Damping Trends for Toy Model vs. Multi-Agent System

6.4 Avoidance Performance

As described in Section 5.1, distances between each and every agents are a measure of avoidance behaviour. In Chapter 4, distances between toy model two-particles are mathematically expressed for both cases with and without anticipation. Distance expressions for these models are tabulated below at Tables 6.2 and 6.3 with highlighted additional terms in order to understand effect of anticipation better.

Table 6.2: Distance between Two-Particles for Head-to-Tail Toy Models

Model	Distance ($\lvert\Delta x_1 - \Delta x_2\rvert$)
1st Order w/o Ant.	$\lvert 2C_2 e^{-2\alpha k t}\rvert$
1st Order w/ Ant.	$\lvert 2C_2 e^{-\frac{2\alpha k}{1+2\alpha b} t}\rvert$
2nd Order w/o Ant.	$2C_2 e^{\frac{-1-\sqrt{1-8\alpha^2 km}}{2\alpha m} t} + 2C_3 e^{\frac{-1+\sqrt{1-8\alpha^2 km}}{2\alpha m} t}$
2nd Order w/ Ant.	$2C_2 e^{\frac{-1-2\alpha b-\sqrt{1-8\alpha^2 km+4\alpha^2 b^2}}{2\alpha m} t} + 2C_3 e^{\frac{-1-2\alpha b+\sqrt{1-8\alpha^2 km+4\alpha^2 b^2}}{2\alpha m} t}$

Table 6.3: Distance between Two-Particles for Side-by-Side Toy Models

Model	Distance ($\lvert 2\Delta y\rvert$)
1st Order w/o Ant.	$\lvert 2C_1 e^{-\sqrt{-2\beta k v_0} t} + 2C_2 e^{\sqrt{-2\beta k v_0} t}\rvert$
1st Order w/ Ant.	$2C_1 e^{\left(-\beta b v_0 - \sqrt{\beta^2 b^2 v_0^2 - 2\beta k v_0}\right) t} + 2C_2 e^{\left(-\beta b v_0 + \sqrt{\beta^2 b^2 v_0^2 - 2\beta k v_0}\right) t}$
2nd Order w/o Ant.	*Long Analytical Solutions*
2nd Order w/ Ant.	*Long Analytical Solutions*

Side-by-side model in 1st order, the one closest to the multi-agent AEAnt, has faster decay rates with the inclusion of anticipation until a critical value as long as all else is kept equal. This is an expected result from Figure 6.3 since anticipation is pictured kinetically analogous to damping.

Avoidance effect is prominent in multi-agent systems as well. Two experimental setups (duct passage and wall bounce) are utilized in order to demonstrate the contribution by anticipation. Both maximum, minimum and average distances between

particles are traced and plotted as a function of each time-step throughout the whole simulation. Figures 6.9 and 6.12 display typical duct passage and wall bounce, respectively. For both scenarios, envelopes for the curves given in Figures 6.10 and 6.13 demonstrate increase in minimum and decrease in maximum distances as anticipation is emphasised. This means that when each curve is bordered with a tangential envelope, absolute values of the peak amplitudes reduce with increasing anticipation. Such effect is even valid for the envelope curves of average distances (see Figures 6.11 and 6.14).

In terms of avoidance, distances become smaller and smaller as a collision occurs. But when the system has anticipation and agents on the back anticipate collision, they do not favour pushing ones in the front and result in an increased minimum distance of the system. An opposite case exists for maximum distance as well. When agents try to disperse, distances become larger and larger as separation occurs. Ones at the circumference anticipate breakaway and do not favour repulsion by the next inner peripheral ring. Therefore, distances are opted for smaller values so that the maximum distance decreases.

Existence of anticipation not only dampens oscillations but also increases avoidance and aggregation performances. Therefore, system adopts more stable and ordered actions which render swarming tasks such as an ordinary duct passage possible. Stability and order characteristics are to be further investigated in the upcoming section, yet Figure 6.15 shows how lack (or insufficient amount) of anticipation can result in a passage failure due to unexpected oscillatory collisions with poor avoidance response.

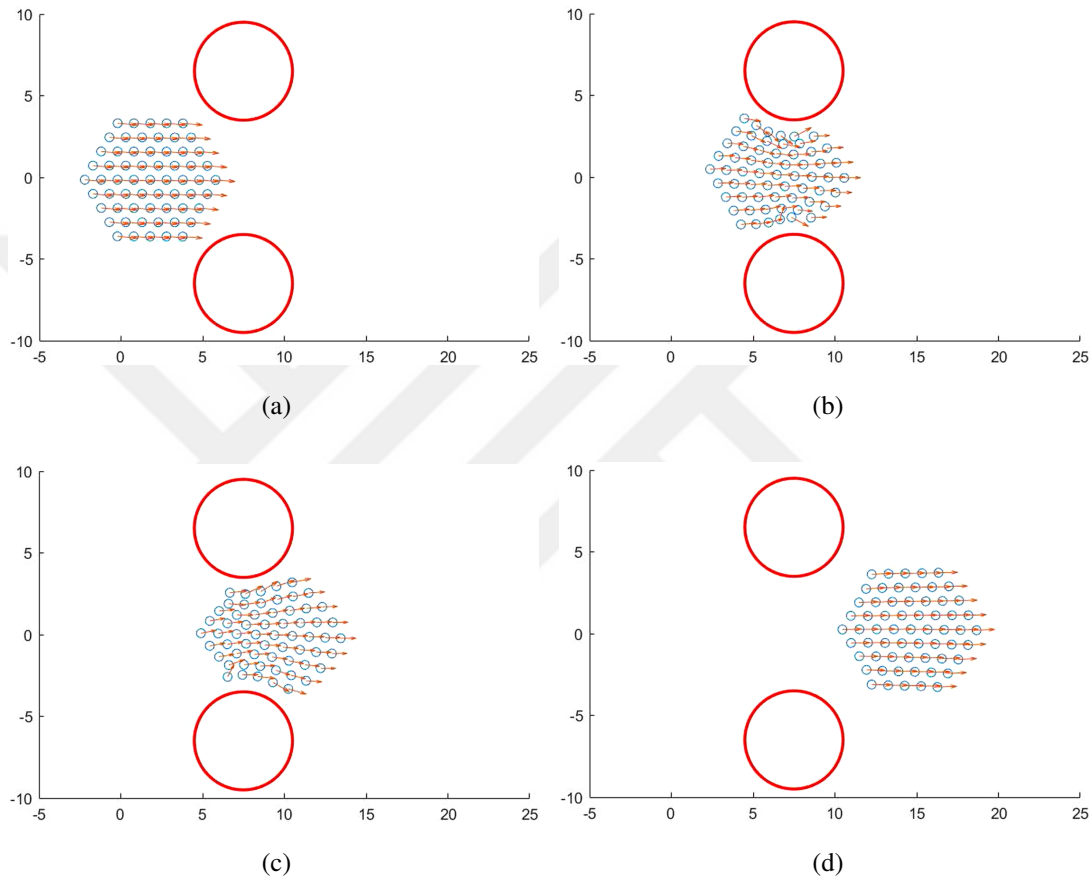

Figure 6.9: Typical Duct Passage

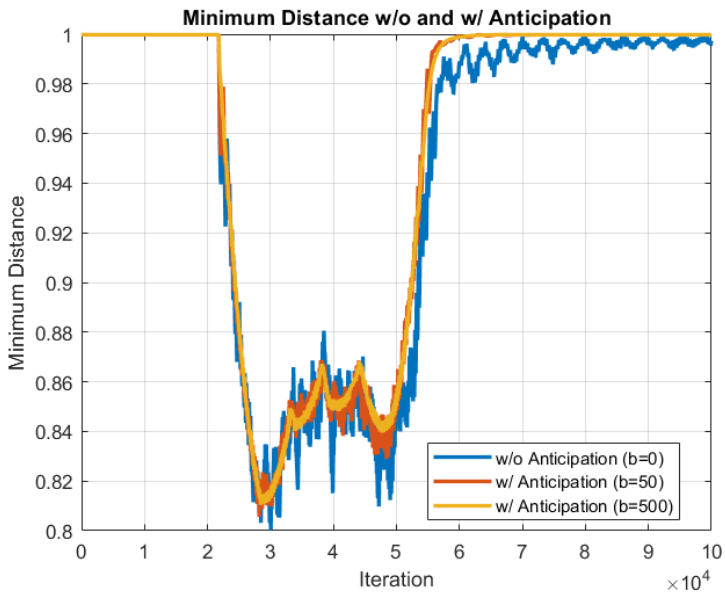

(a) Minimum Distance Plot

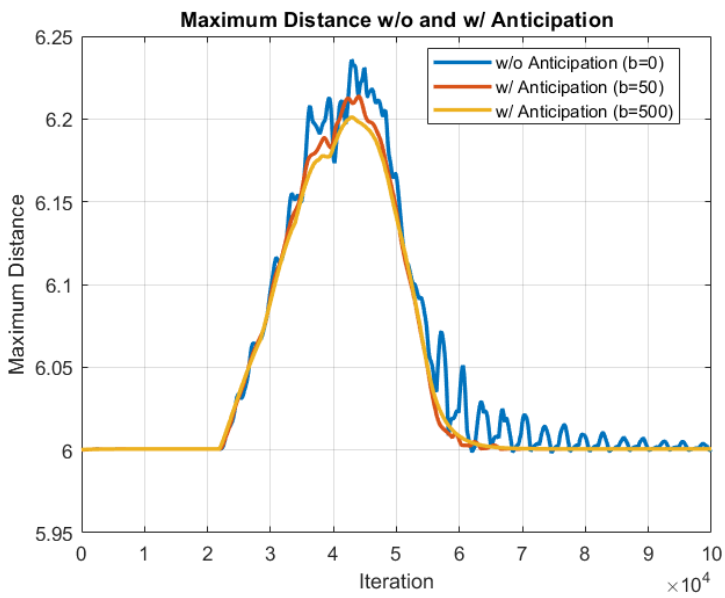

(b) Maximum Distance Plot

Figure 6.10: Minimum and Maximum Distances in a Typical Duct Passage

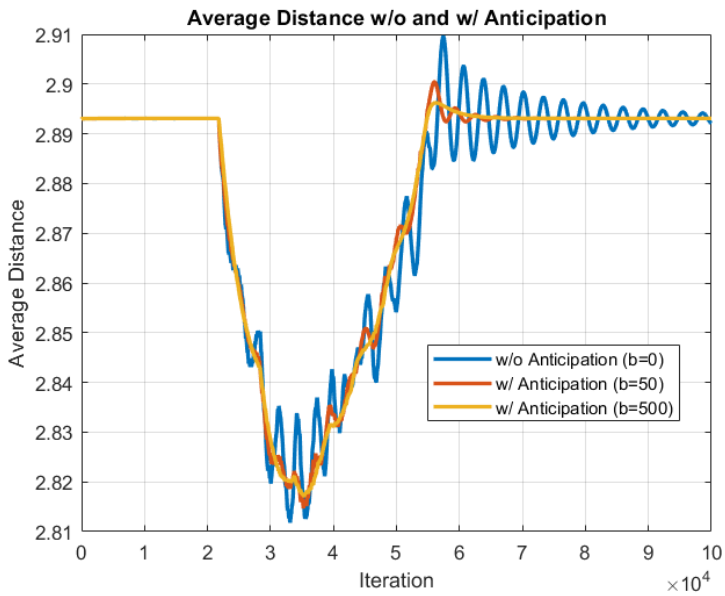

Figure 6.11: Average Distance in a Typical Duct Passage

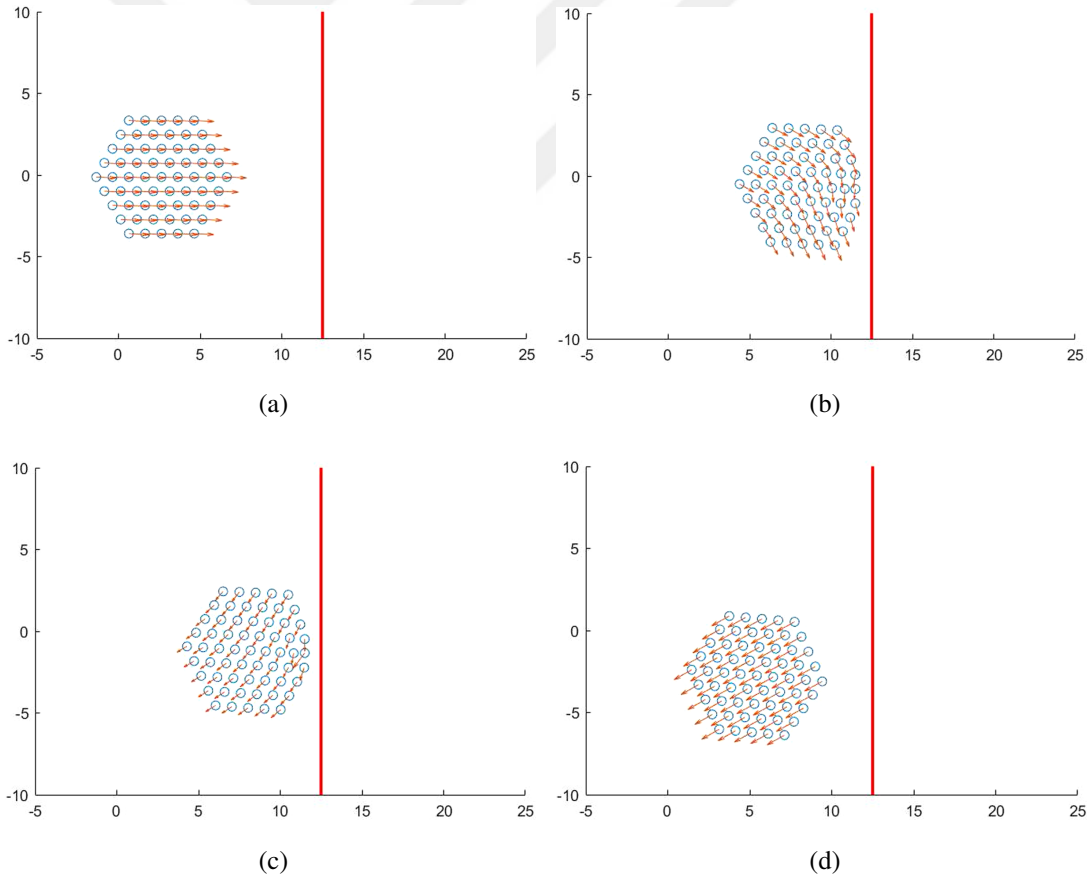

Figure 6.12: Typical Wall Bounce

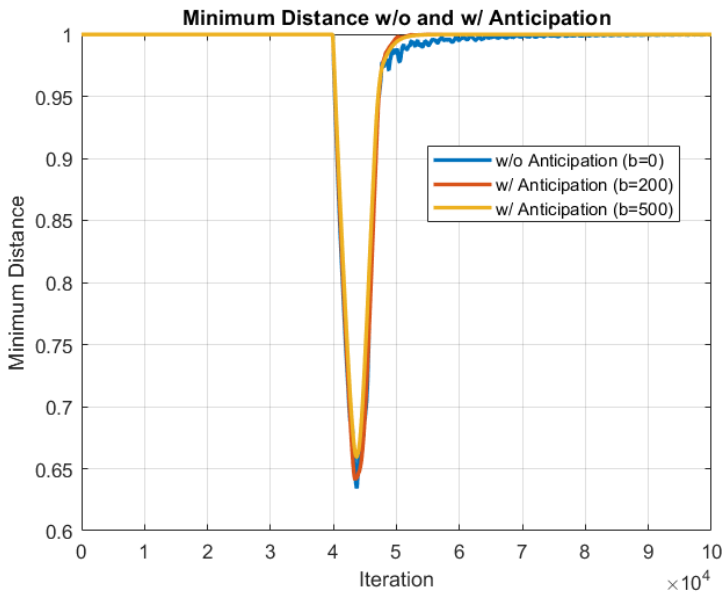

(a) Minimum Distance Plot

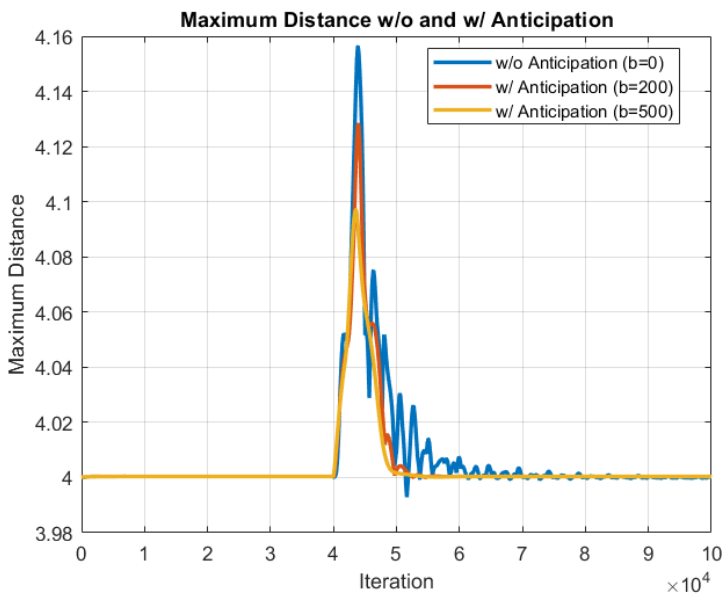

(b) Maximum Distance Plot

Figure 6.13: Minimum and Maximum Distances in a Typical Wall Bounce

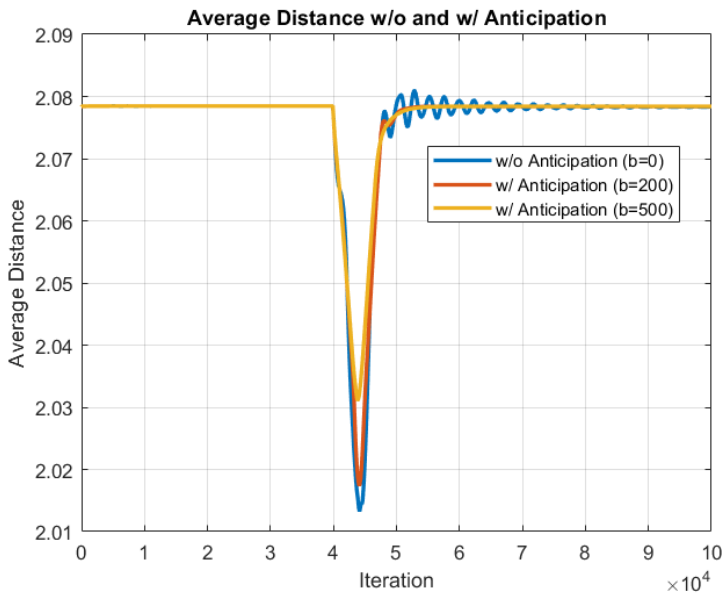

Figure 6.14: Average Distance in a Typical Wall Bounce

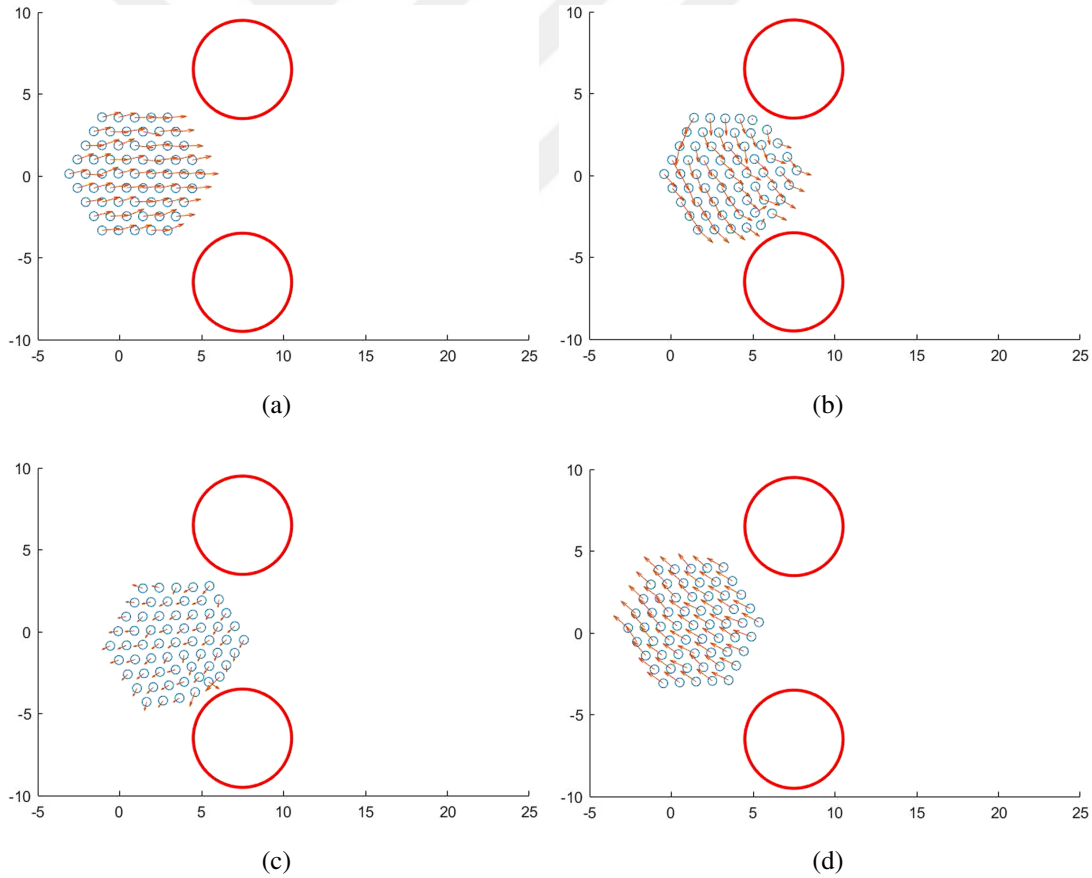

Figure 6.15: Duct Passage Failure

6.5 Phase Diagrams

As how control systems are susceptible to noise, a similar phenomenon exists for AM systems where there is a critical value above which an order-disorder transition occurs. Phase diagrams are utilized so as to study such transitions in matters. Similarly, robotic systems can have homologous order-disorder transitions after a certain amount of noise introduced to the system. In that sense, studying phase diagrams for multi-agent systems is valuable for better performance measures in swarm robotics applications. Such diagrams are already studied by [1, 2, 25–27, 47]. In this section, similar studies are carried out with the addition of anticipation and inertia.

All phase diagrams are plotted as polarization (order parameter) vs. actuation noise strength coefficient in accordance with the Section 5.1. To start with, a triangular lattice under hexagonal formation with a side length of 7 is placed in a confined arena with periodic boundary conditions. This means 127 agents are located at the centre of an arena with initial random heading directions, and actuation noise strength is gradually increased as order is traced for each time instant. The Figure 6.16 below demonstrates how existence of anticipation shifts order-disorder transition to the right. It is also observed that existence of anticipation changes transition behaviour from first-order-like to second-order-like just similar to the cases studied in [2, 25–27, 47]. It is to be noted that each and every data point in transition plots corresponds to a single run of the complete simulation.

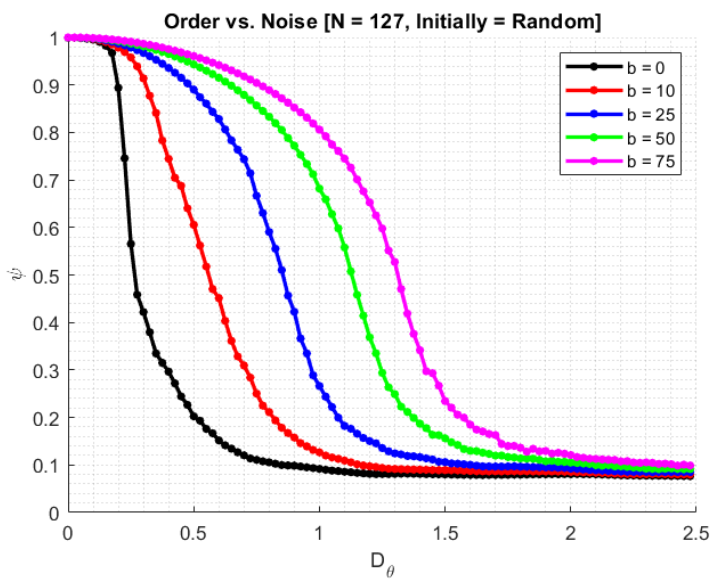

Figure 6.16: Order vs. Noise for Different Anticipation Values with $N = 127$ and Initially: Random

It is also to be argued that introduction of random angular orientations in the beginning may result in an altered behaviour. Figure 6.17 shows how this phase transition is more related to fundamental configurations rather than initially introduced ordered/disordered heading directions.

System size plays a great role in order-disorder transitions. Unlike AM systems with monumental amount of agents, more sounded counts are taken into consideration for a better engineering perspective. For that matter, it is studied whether nearly doubling the system size would change order characteristics of the ensemble. Side length of 10 with 271 agents are compared to the previous case. It is again seen in Figure 6.18 that the swarm polarization is not altered drastically unless system size changes in order of magnitudes by means of scale. Increase in the system size would make transition more discontinuous under normal circumstances. This is expected since ideal transition in an infinite system does not happen in a continuous manner. To that extent, change in Figure 6.18 according to system size is shaped such that it becomes more discontinuous with timely flattened bottom levels for higher amount of agents.

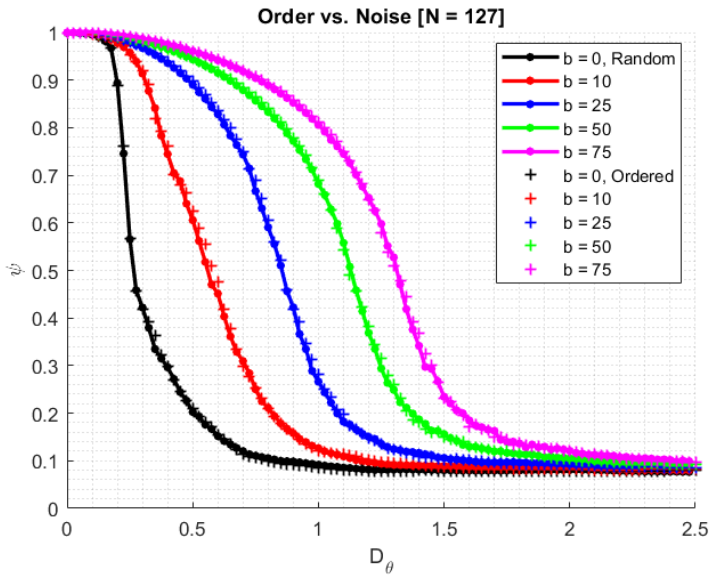

Figure 6.17: Order vs. Noise for Different Anticipation Values with $N = 127$ and Initially: Random vs. Ordered

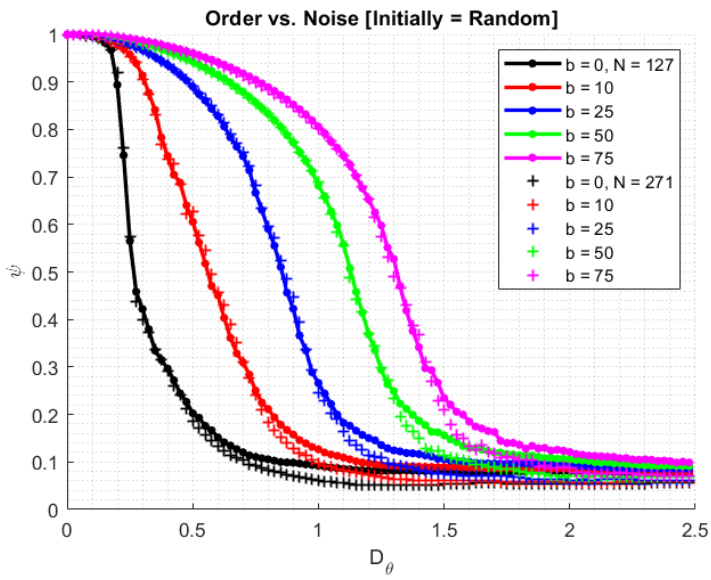

Figure 6.18: Order vs. Noise for Different Anticipation Values with $N = 127$ vs. $N = 271$ and Initially: Random

6.5.1 Phase Diagrams with Inertial Effects

The last but not least parameter to be studied in phase diagrams is the inclusion of inertia. In toy models, two inertial parameters are introduced, namely mass and rotational inertia. Tuning mass in multi-agent systems is more challenging as translational equation-of-motion includes self-propulsion speed which is artificially coupled to the dynamics. Therefore, only rotational inertia is studied in terms of agent orientations as angular equation of motion is more trivial and intuitive.

The Figure 6.19a below demonstrates how existence of rotational inertia shifts order-disorder transition to the left. It is also observed that the existence of inertia changes transition behaviour from second-order-like to first-order-like. The reason for this inverse effect is that system cannot justify alterations by the noise as their response drastically slows down.

As a composite way of interpreting rotational inertia with anticipation, the same configuration with different b values are plotted at Figures 6.19b,6.19c and 6.19d below. It is seen that amount of anticipation can drastically shift all inertia curves to the right.

The more inertial system becomes, the more ineffective how anticipation is utilized. The main motivation behind anticipating the neighbouring agents becomes laggy by means of performance due to slow system response. Yet, it is valuable to observe that anticipating more can compensate susceptibility to noise by again shifting transition points to the right despite inclusion of the inertia. This is demonstrated by Figure 6.20 under different rotational inertia values below. Yet, Figure 6.21 proves the limits for such an effect by further doubling the rotational inertia value from Figure 6.20d in order to show how almost the same polarization curve is achieved regardless of the anticipation value.

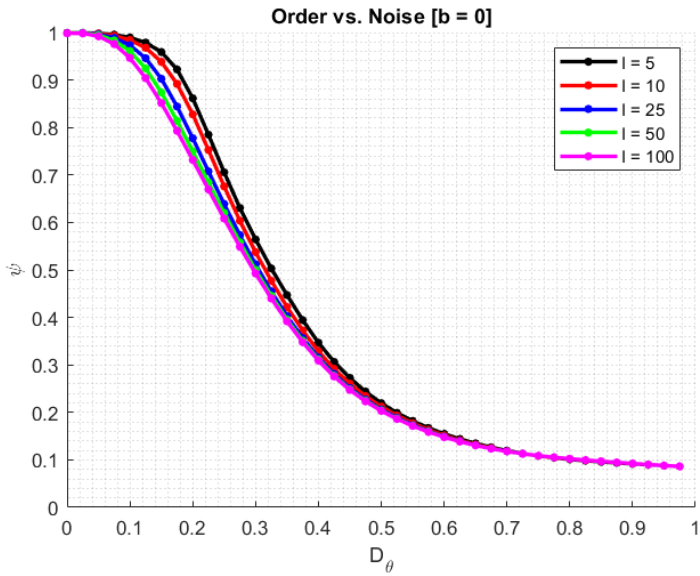

(a) Order vs. Noise with $b = 0$ for Different Rotational Inertia Values

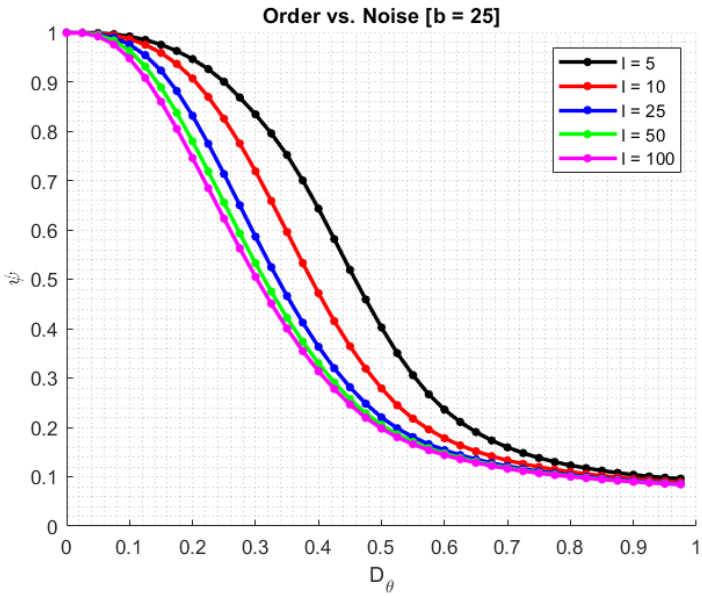

(b) Order vs. Noise with $b = 25$ for Different Rotational Inertia Values

Figure 6.19: Order vs. Noise with Various Anticipation Degrees for Different Rotational Inertia Values

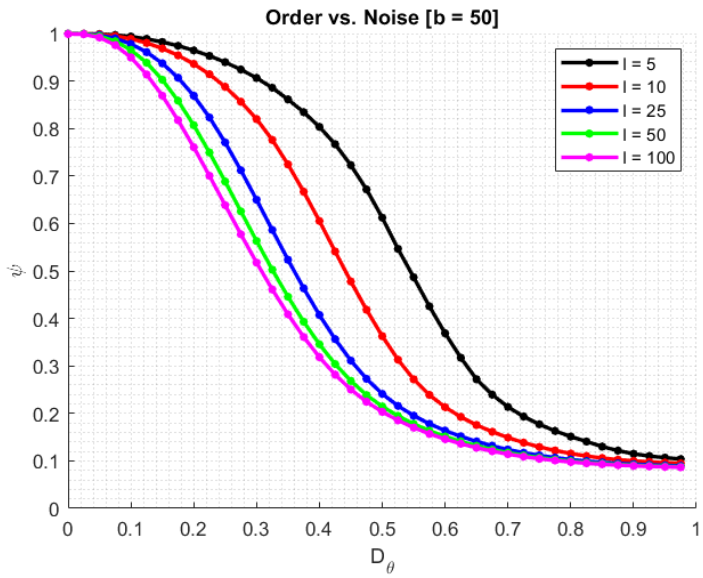

(c) Order vs. Noise with $b = 50$ for Different Rotational Inertia Values

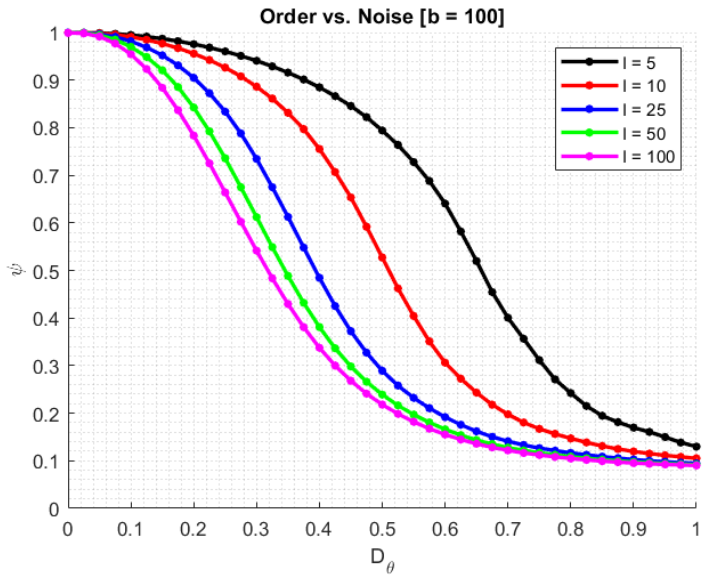

(d) Order vs. Noise with $b = 100$ for Different Rotational Inertia Values

Figure 6.19: Order vs. Noise with Various Anticipation Degrees for Different Rotational Inertia Values (Cont.)

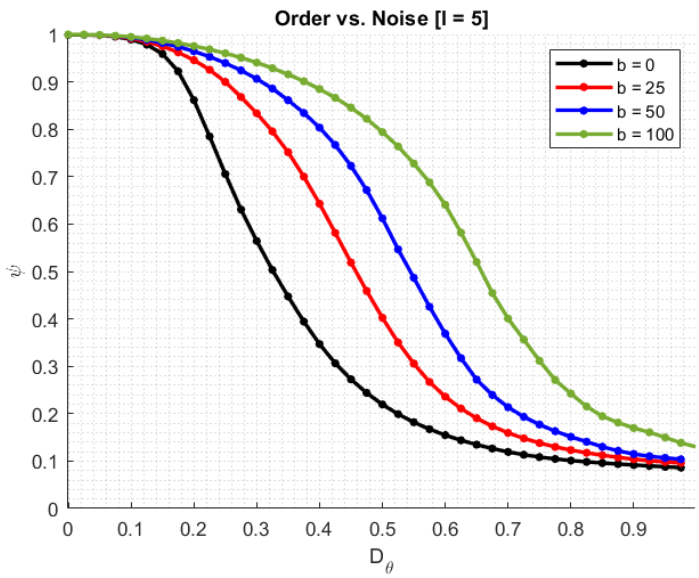

(a) Order vs. Noise with $I = 5$ for Different Anticipation Values

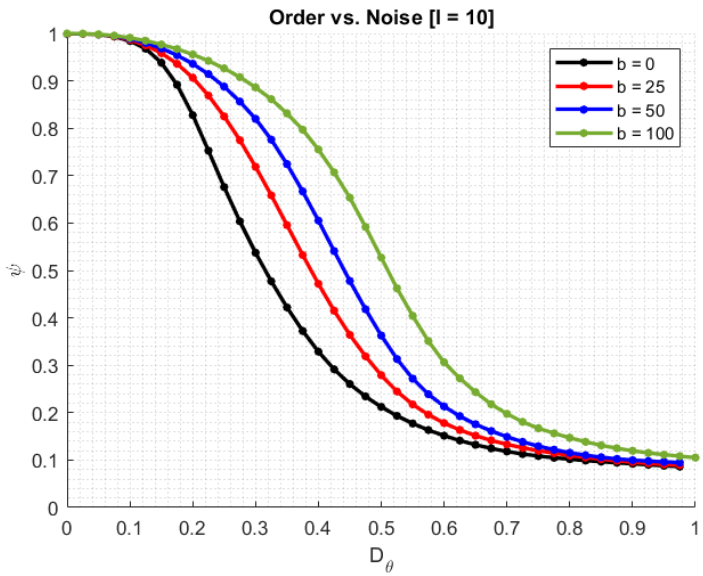

(b) Order vs. Noise with $I = 10$ for Different Anticipation Values

Figure 6.20: Order vs. Noise with Various Rotational Inertia Values for Different Anticipation Degrees

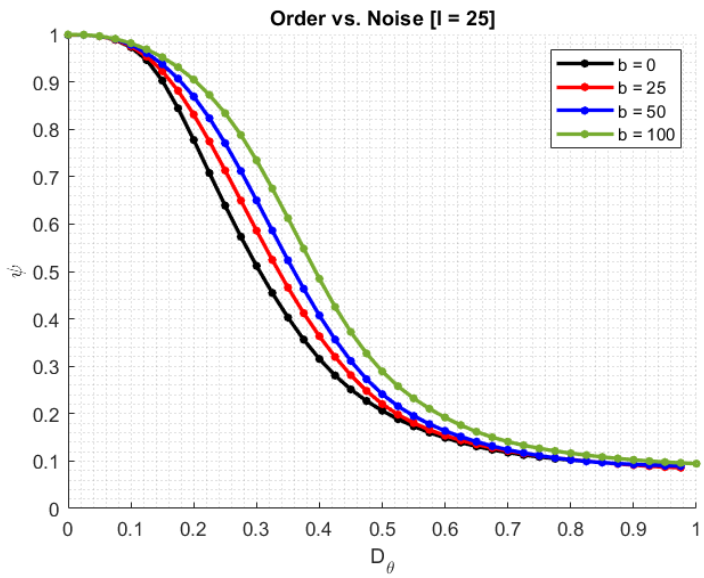

(c) Order vs. Noise with $I = 25$ for Different Anticipation Values

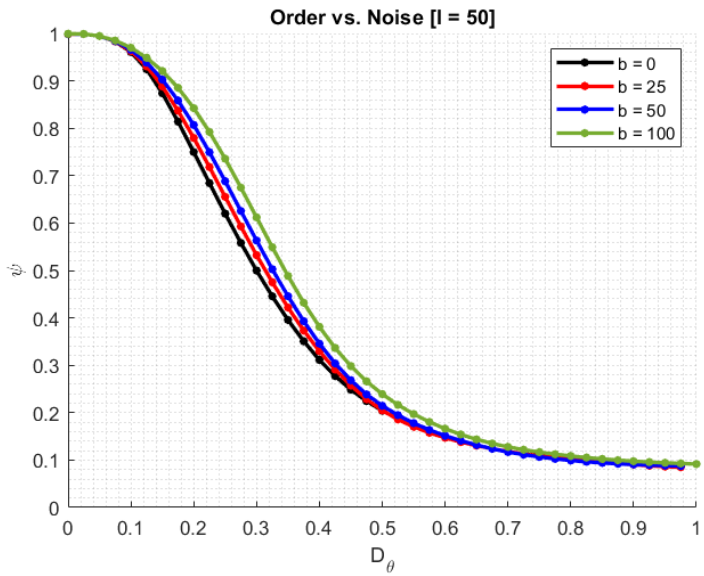

(d) Order vs. Noise with $I = 50$ for Different Anticipation Values

Figure 6.20: Order vs. Noise with Various Rotational Inertia Values for Different Anticipation Degrees (Cont.)

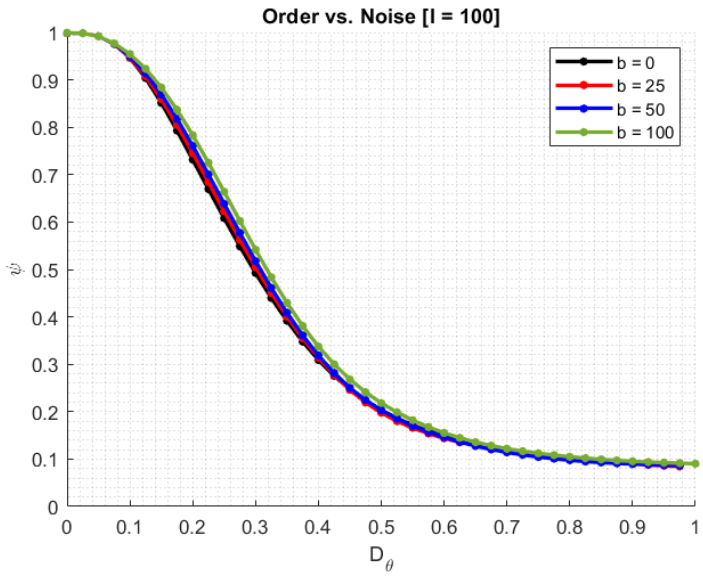

Figure 6.21: Order vs. Noise with $I = 100$ for Different Anticipation Values

CHAPTER 7

CONCLUSION

AE models are simple yet powerful tools with a great potential in swarm robotics applications. In this thesis, AEAnt models are developed with multiple configurations for the purpose of investigating parameters with *downward causation* scaling down to two-particle systems. Mathematical equivalency of AEA and AEAnt is demonstrated for a better conceptualization of what anticipation physically means. It is observed that side-by-side configuration in 1st order promises an anticipation value analogous to critical damping in harmonic oscillators. This is specifically in line with common control performance metrics in order to assess and tune system response. The linear trend of increasing decay rate is justified by making use of the generated multi-agents simulator. With a similar motivation for emergent properties, distances between agents for both toy models and multi-agent systems are compared. It turns out that degree of anticipation enhances avoidance and sticking together by faster decaying responses up to a critical value, if not promised by the harmonic oscillator analogy. Above such a critical value, agents become more and more meticulous so that the ensemble slows down as a whole.

Toy model studies are followed by order-disorder phase transitions for the purpose of noise susceptibility assessments. It turns out that anticipation increases noise resilience by moving transition to a higher actuation noise strength region, similar to the study of AEA by Lin et al. [2] in which similar effect is prominent when R (length of the arm) increases. Hence, equivalency claim between AEA and AEAnt is strengthened by the similar effects on transitions. It is also showed that system size and initial heading direction configuration have minimal effects on transitions shifted due to the presence of anticipation. An opposite influence is observed when rotational inertia

is selected to be the control parameter. Curvy trajectories favoured by rotational inertia would work against anticipation, whereas spatial mass would enhance agents dedication to move towards their anticipated next position. Yet, self-propulsion introduces additional dynamics which makes tuning spatial inertia challenging. Since self-propulsion creates another time-scale, there could be different stable regimes of spatial mass for which a parameter search must be performed. It is still worthwhile to see how robots' rotational inertias are related to swarms' noise acceptance level.

7.1 Future Work

Future work as a follow-up to this thesis is listed below.

- Emergent inertial properties from toy models to multi-agent systems are still open to discovery for similar trends. The linear behaviour of real eigenvalues by side-by-side configuration in 1st order are followed by non-linear trends which could not be demonstrated for multi-agent system due to numerical instabilities. More precision in time increment would solve the issue, yet by drastically boosting simulation time. Finding a parameter space region for which linear to non-linear trend transition occurs and matching both slopes and scales in values are left as a future work.

- Avoidance performance can be investigated for the case with existence of inertia. Since dynamic relaxation by the proportional velocity controller opens the similarity gap between AEAnt and simple form by AES, this thesis focuses purely on anticipation effects only.

- Order-disorder phase transitions as a function of spatial mass are left to be studied in the future due to inferring forward biasing speed in translational equations of motion. It is expected that a parameter selection by fine tuning could enable a region for spatial mass so that similar transition studies can be performed.

- A physical experiment is still left missing with either two-wheeled robots or drones for real robotics applications. It would be valuable to observe how

highly manoeuvrable Crazyflies and relatively more inertial ground robots correspond to the founding by order-disorder transition studies.

- Throughout the thesis, networking topology of *NN:* Nearest Neighbour is set as default. For further exercises, a boolean flag for dynamic networking is enabled within the multi-agent simulator. Further connectivity types such as *ER:* Erdös–Rényi, *SF:* Scale-Free and super-positions of all these are open to similar studies by that of this thesis. One can refer to Turgut et al. [27] for different networking topologies.

REFERENCES

[1] Y. Zheng, C. Huepe, and Z. Han, "Experimental capabilities and limitations of a position-based control algorithm for swarm robotics," *Adaptive Behavior*, vol. 30, no. 1, pp. 19–35, 2022.

[2] G. Lin, Z. Han, and C. Huepe, "Order-disorder transitions in a minimal model of active elasticity," *New Journal of Physics*, vol. 23, no. 2, 2021.

[3] P. Gerlee, K. Tunstrøm, T. Lundh, and B. Wennberg, "Impact of anticipation in dynamical systems," *Physical Review E*, vol. 96, no. 6, pp. 1–11, 2017.

[4] T. Ritchey, "On a Morphology of Theories of Emergence," *Acta Morphologica Generalis*, vol. 3, no. 3, pp. 1–16, 2014.

[5] R. Aditi Simha and S. Ramaswamy, "Hydrodynamic fluctuations and instabilities in ordered suspensions of self-propelled particles," *Physical review letters*, vol. 89, no. 5, p. 058101, 2002.

[6] T. Vicsek, A. Czirók, E. Ben-Jacob, I. Cohen, and O. Shochet, "Novel Type of Phase Transition in a System of Self-Driven Particles," *Physical Review Letters*, vol. 75, pp. 1226–1229, aug 1995.

[7] M. Aldana and C. Huepe, "Phase Transitions in Self-Driven Many-Particle Systems and Related Non-Equilibrium Models: A Network Approach," *Journal of Statistical Physics*, vol. 112, no. 1-2, pp. 135–153, 2003.

[8] G. Grégoire and H. Chaté, "Onset of Collective and Cohesive Motion," *Physical Review Letters*, vol. 92, no. 2, p. 4, 2004.

[9] H. Chaté, F. Ginelli, G. Grégoire, and F. Raynaud, "Collective motion of self-propelled particles interacting without cohesion," *Physical Review E - Statistical, Nonlinear, and Soft Matter Physics*, vol. 77, no. 4, pp. 1–15, 2008.

[10] A. M. Menzel and H. Löwen, "Traveling and resting crystals in active systems," *Physical Review Letters*, vol. 110, no. 5, pp. 1–5, 2013.

[11] B. Szabó, G. J. Szöllösi, B. Gönci, Z. Jurányi, D. Selmeczi, and T. Vicsek, "Phase transition in the collective migration of tissue cells: Experiment and model," *Physical Review E - Statistical, Nonlinear, and Soft Matter Physics*, vol. 74, no. 6, pp. 1–5, 2006.

[12] A. Peshkov, S. Ngo, E. Bertin, H. Chaté, and F. Ginelli, "Continuous theory of active matter systems with metric-free interactions," *Physical Review Letters*, vol. 109, no. 9, pp. 1–6, 2012.

[13] J. Fromm, *The Emergence of Complexity*. Kassel University Press, 2004.

[14] C. W. Reynolds, "Flocks, herds, and schools: A distributed behavioral model," *Proceedings of the 14th Annual Conference on Computer Graphics and Interactive Techniques, SIGGRAPH 1987*, vol. 21, no. 4, pp. 25–34, 1987.

[15] G. Grégoire, H. Chaté, and Y. Tu, "Moving and staying together without a leader," *Physica D: Nonlinear Phenomena*, vol. 181, no. 3-4, pp. 157–170, 2003.

[16] P. Romanczuk, I. D. Couzin, and L. Schimansky-Geier, "Collective motion due to individual escape and pursuit response," *Physical Review Letters*, vol. 102, no. 1, pp. 1–4, 2009.

[17] T. Vicsek and A. Zafeiris, "Collective motion," *Physics Reports*, vol. 517, no. 3-4, pp. 71–140, 2012.

[18] M. Fleischer, "Foundations of Swarm Intelligence: From Principles to Practice," *Conference on Swarming and Network Enabled C4ISR*, 2005.

[19] M. Schranz, G. A. Di Caro, T. Schmickl, W. Elmenreich, F. Arvin, A. Sekercioglu, and M. Sende, "Swarm Intelligence and cyber-physical systems: Concepts, challenges and future trends," *Swarm and Evolutionary Computation*, vol. 60, no. October 2019, 2021.

[20] N. Fernández, C. Maldonado, and C. Gershenson, "Information Measures of Complexity, Emergence, Self-organization, Homeostasis, and Autopoiesis," in *Guided Self-Organization: Inception. Emergence, Complexity and Computation*, vol. 9, pp. 19–51, Springer, Berlin, Heidelberg, 2014.

[21] F. Boschetti, M. Prokopenko, I. Macreadie, and A. M. Grisogono, "Defining and detecting emergence in complex networks," *Lecture Notes in Computer Science (including subseries Lecture Notes in Artificial Intelligence and Lecture Notes in Bioinformatics)*, vol. 3684 LNAI, no. September, pp. 573–580, 2005.

[22] Y. Katz, K. Tunstrøm, C. C. Ioannou, C. Huepe, and I. D. Couzin, "Inferring the structure and dynamics of interactions in schooling fish," *Proceedings of the National Academy of Sciences of the United States of America*, vol. 108, no. 46, pp. 18720–18725, 2011.

[23] W. Bialek, A. Cavagna, I. Giardina, T. Mora, E. Silvestri, M. Viale, and A. M. Walczak, "Statistical mechanics for natural flocks of birds," *Proceedings of the National Academy of Sciences of the United States of America*, vol. 109, no. 13, pp. 4786–4791, 2012.

[24] D. Grossman, I. S. Aranson, and E. Ben Jacob, "Emergence of agent swarm migration and vortex formation through inelastic collisions," *New Journal of Physics*, vol. 10, 2008.

[25] E. Ferrante, A. E. Turgut, M. Dorigo, and C. Huepe, "Elasticity-based mechanism for the collective motion of self-propelled particles with springlike interactions: A model system for natural and artificial swarms," *Physical Review Letters*, vol. 111, no. 26, 2013.

[26] E. Ferrante, A. E. Turgut, M. Dorigo, and C. Huepe, "Collective motion dynamics of active solids and active crystals," *New Journal of Physics*, vol. 15, 2013.

[27] A. E. Turgut, I. C. Boz, I. E. Okay, E. Ferrante, and C. Huepe, "Interaction network effects on position- and velocity-based models of collective motion," *Journal of the Royal Society Interface*, vol. 17, no. 169, 2020.

[28] Y. Mohan and S. G. Ponnambalam, "An extensive review of research in swarm robotics," *2009 World Congress on Nature and Biologically Inspired Computing, NABIC 2009 - Proceedings*, no. January, pp. 140–145, 2009.

[29] M. Brambilla, E. Ferrante, M. Birattari, and M. Dorigo, "Swarm robotics: A

review from the swarm engineering perspective," *Swarm Intelligence*, vol. 7, no. 1, pp. 1–41, 2013.

[30] J. C. Barca and A. Sekercioglu, "Swarm robotics reviewed," *Robotica*, vol. 31, no. 3, pp. 345–359, 2013.

[31] Y. Tan and Z. yang Zheng, "Research Advance in Swarm Robotics," *Defence Technology*, vol. 9, no. 1, pp. 18–39, 2013.

[32] I. Navarro and F. Matía, "An Introduction to Swarm Robotics," *ISRN Robotics*, vol. 2013, pp. 1–10, 2013.

[33] L. Bayindir, "A review of swarm robotics tasks," *Neurocomputing*, vol. 172, no. February, pp. 292–321, 2016.

[34] J. Gomes, P. Urbano, and A. L. Christensen, "Evolution of swarm robotics systems with novelty search," *Swarm Intelligence*, vol. 7, no. 2-3, pp. 115–144, 2013.

[35] V. Trianni, E. Tuci, C. Ampatzis, and M. Dorigo, "Evolutionary Swarm Robotics: A Theoretical and Methodological Itinerary from Individual Neurocontrollers to Collective Behaviors," *The Horizons of Evolutionary Robotics*, pp. 1–15, 2019.

[36] M. Gauci, J. Chen, W. Li, T. J. Dodd, and R. Groß, "Self-organized aggregation without computation," *International Journal of Robotics Research*, vol. 33, no. 8, pp. 1145–1161, 2014.

[37] M. Gauci, J. Chen, W. Li, T. J. Dodd, and R. Groß, "Clustering objects with robots that do not compute," *13th International Conference on Autonomous Agents and Multiagent Systems, AAMAS 2014*, vol. 1, no. January, pp. 421–428, 2014.

[38] W. Li, M. Gauci, and R. Groß, "Turing learning: a metric-free approach to inferring behavior and its application to swarms," *Swarm Intelligence*, vol. 10, no. 3, pp. 211–243, 2016.

[39] R. Groß, Y. Gu, W. Li, and M. Gauci, "Generalizing GANs: A turing perspective," *Advances in Neural Information Processing Systems*, vol. 2017-Decem, no. Nips, pp. 6317–6327, 2017.

[40] Y. Gu, W. Li, and R. Groß, "Turing learning with hybrid discriminators: Combining the best of active and passive learning," *GECCO 2020 Companion - Proceedings of the 2020 Genetic and Evolutionary Computation Conference Companion*, pp. 121–122, 2020.

[41] E. Ferrante, A. E. Turgut, A. Stranieri, and C. Pinciroli, "Self-Organized Flocking with a Mobile Robot Swarm : a Novel Motion Control Method," *Adaptive Behavior*, vol. 20, no. 6, pp. 460–477, 2012.

[42] K. N. McGuire, C. de Wagter, K. Tuyls, H. J. Kappen, and G. C. de Croon, "Minimal navigation solution for a swarm of tiny flying robots to explore an unknown environment," *Science Robotics*, vol. 4, no. 35, 2019.

[43] E. Soria, F. Schiano, and D. Floreano, "Predictive control of aerial swarms in cluttered environments," *Nature Machine Intelligence*, vol. 3, no. 6, pp. 545–554, 2021.

[44] M. Raoufi, A. E. Turgut, and F. Arvin, "Self-organized Collective Motion with a Simulated Real Robot Swarm," *Towards Autonomous Robotic Systems (TAROS)*, 2019.

[45] A. Czirók and T. Vicsek, "Collective motion," *Statistical Mechanics of Biocomplexity*, no. March 2016, pp. 152–164, 2008.

[46] M. Bando, K. Hasebe, K. Nakanishi, A. Nakayama, A. Shibata, and Y. Sugiyama, "Phenomenological Study of Dynamical Model of Traffic Flow," *Journal de Physique I*, vol. 5, no. 11, pp. 1389–1399, 1995.

[47] E. Ferrante, A. E. Turgut, M. Dorigo, and C. Huepe, "Elasticity-based mechanism for the collective motion of self-propelled particles with springlike interactions: A model system for natural and artificial swarms," *Physical Review Letters*, vol. 111, no. 26, 2013.